Transport Model for Relativistic Nuclear Collisions

Zi-Wei Lin (林子威)
East Carolina University (ECU)

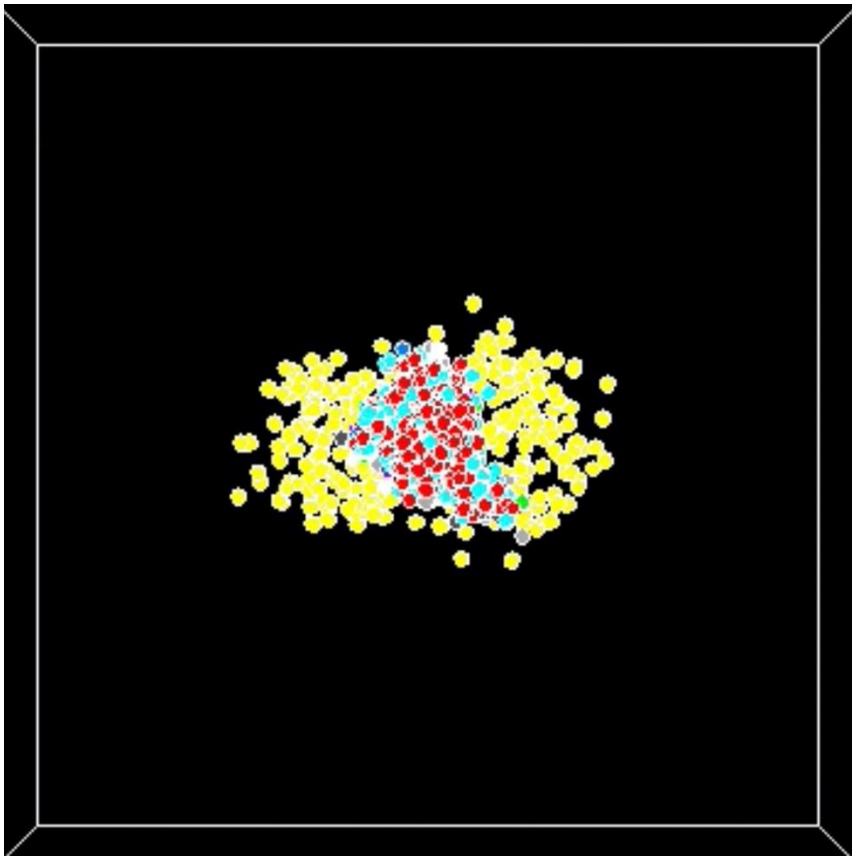

Outline

- Introduction
- Structure of a Multi-phase Transport (AMPT) Model
- Selected results
  including a detailed discussion on the escape mechanism
- Challenges & opportunities

Major goals of relativistic heavy ion collisions

- Explore the QCD phase diagram:
  Order/temperature of deconfinement transition,
  Whether a critical endpoint (CEP) exist, EoS, ...

- Study of deconfinement transition / QGP properties:
  shear & bulk viscosities,
  thermalization of different flavors, ...

- Study of confinement transition / hadronization:
  Cooper-Frye / viscous corrections,
  Quark coalescence / parton recombination / valon model, …

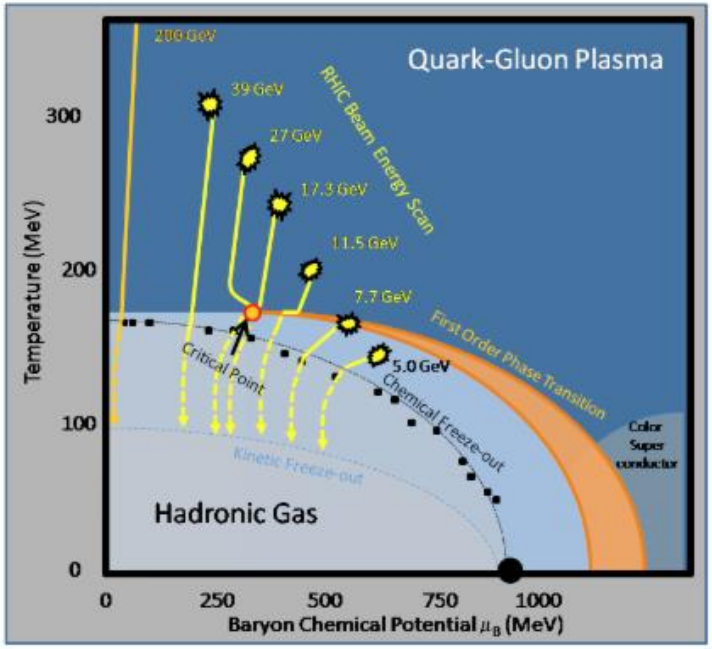

from STAR
arXiv:1007.2613

- Exotic/surprise findings:
  Anti-(hyper)nuclei, vorticity and polarization,
  Chiral magnetic effects?
  Effects from electromagnetic fields? …

Transport models have been developed to study and simulate high energy heavy ion collisions.

They can be
classical transport mostly based on the Boltzmann equation
or
quantum transport (for example, for spin or chiral transport)

See lectures from ZHUANG Pengfei, LIN Shu,
LIAO Jinfeng, and HOU Defu at this summer school.

Classical transport models include

ART, HSD, UrQMD, SMASH (hadron transport)

ZPC, MPC (elastic parton transport)

AMPT (elastic parton transport + hadron transport)

PACIAE (2-body parton transport + hadron transport)

BAMPS (2-body plus $2 \leftrightarrow 3$ parton transport)

PHSD (off-shell parton transport + hadron transport)

...

Not included in here:

Event generators without final state rescatterings:
PYTHIA, HIJING, ...

Hydrodynamics or hybrid (hydrod+hadron transport) models:
EPOS, JAM, VISHNU, ...

From now on, I will use the AMPT model
to illustrate some features of a classical transport model.

A multi-phase transport (AMPT) model
aims to provide a kinetic description of all essential stages
of relativistic heavy ion collisions:

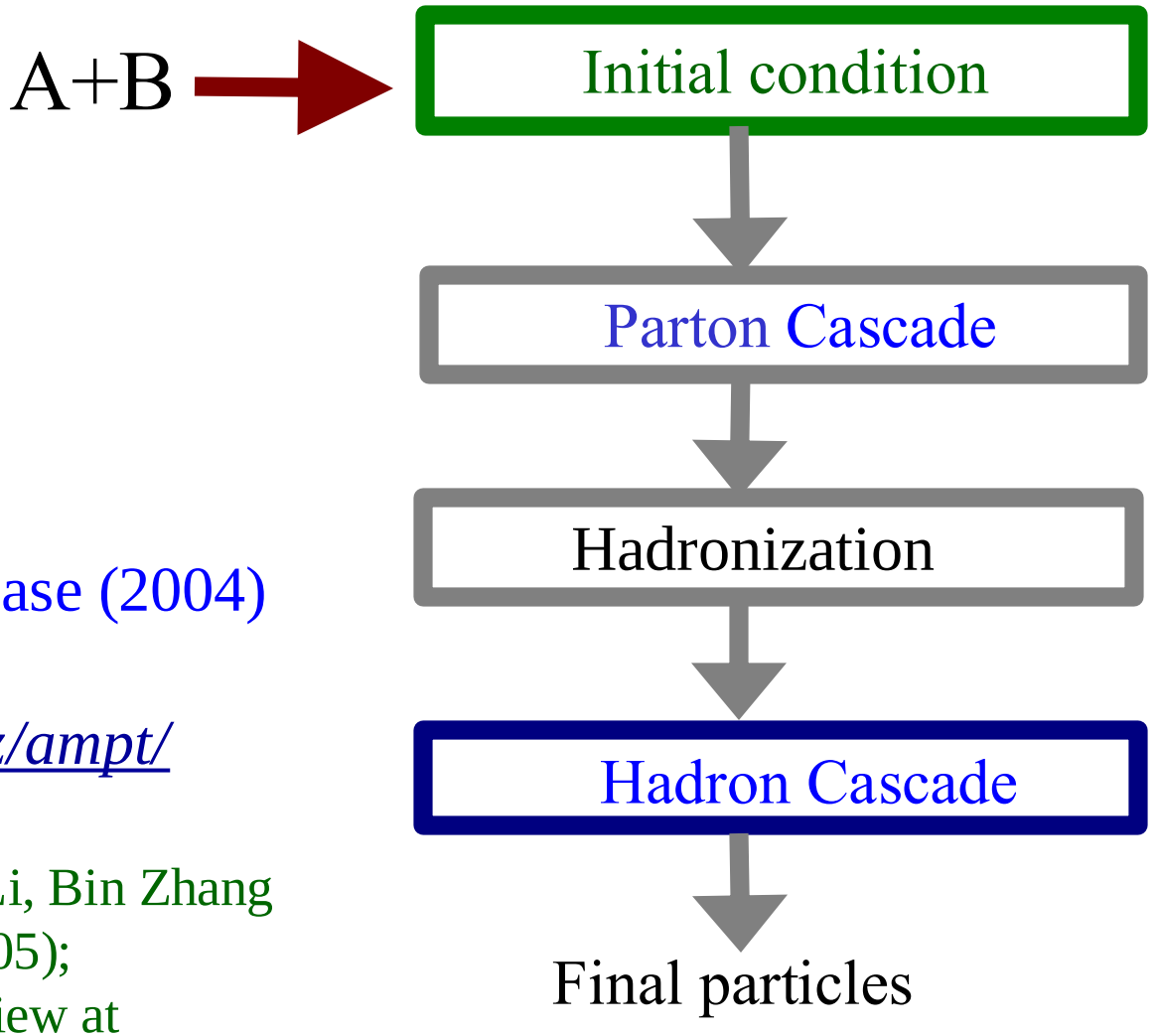

Source codes since 1st release (2004)
are available at
https://myweb.ecu.edu/linz/ampt/

ZWL, Che-Ming Ko, Bao-An Li, Bin Zhang
& Subrata Pal, Phys Rev C (2005);
ZWL & Liang Zheng, mini-review at
Nucl Sci Tech (2021)

For comprehensive simulations of high energy heavy ion collisions

We need:	**Choices:**
Initial particle/energy production	***Soft+hard model (& string melting)***, *CGC, pQCD, Lund strings, ...*
Pre-equilibrium interactions: *equilibration, thermalization, pre-flow*	*Parton cascade (**ZPC**, MPC, BAMPS), CGC, AdS/CFT, ...*
Space-time evolution of QGP	*Parton cascade (**ZPC**, MPC, BAMPS), (ideal or viscous) hydrodynamics, ...*
Hadronization /QCD phase transition	***Quark coalescence/parton recombination, fragmentation**, Cooper-Frye, statistical hadronization, rate equations, ...*
Hadronic interactions	*Hadron cascade (**ART**, UrQMD, SMASH), ...*

The AMPT model currently includes the ***green*** components for each stage.

Structure of AMPT v1.xx (Default version)

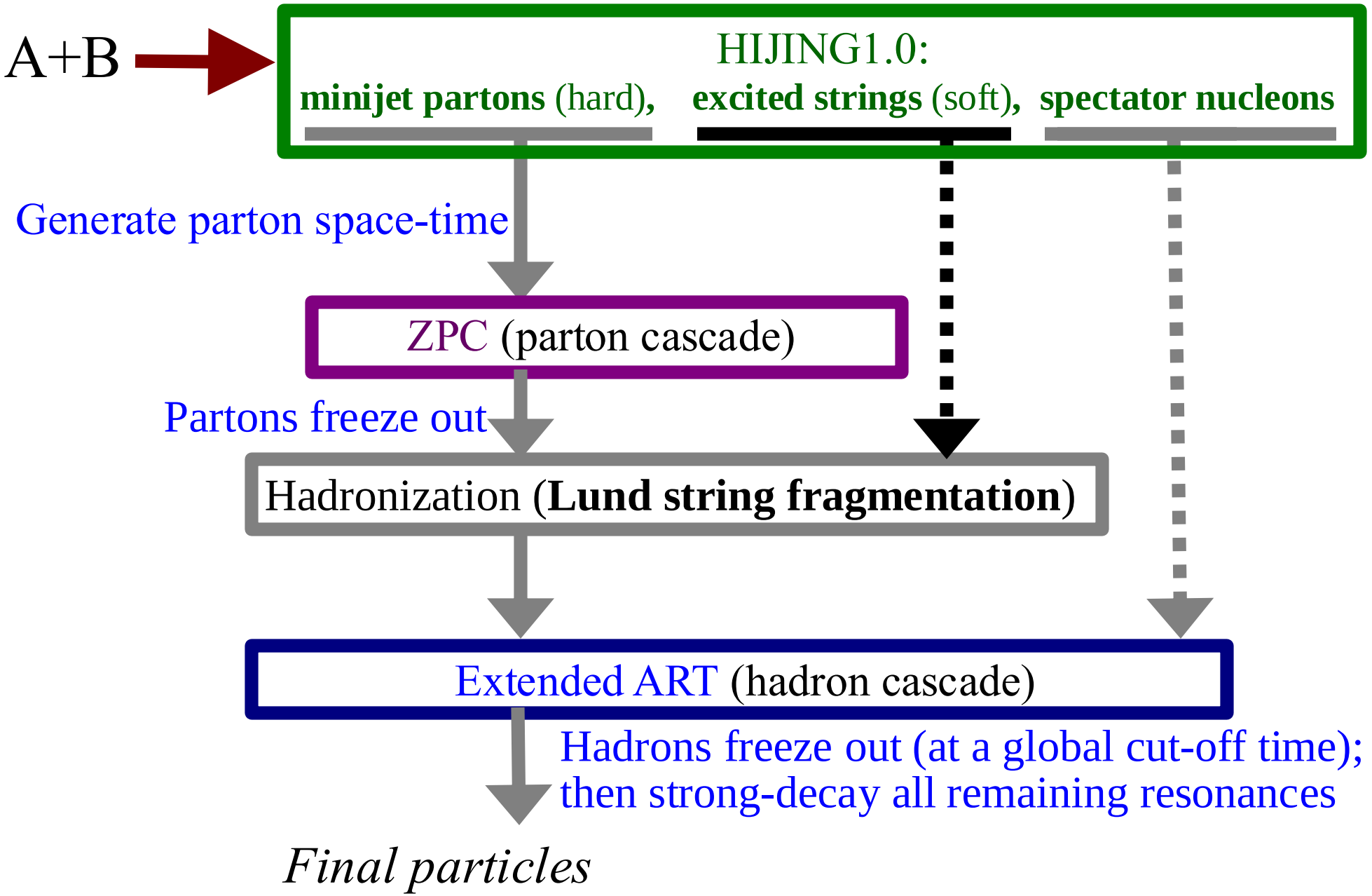

A central Au+Au event at 200AGeV from the Default AMPT model

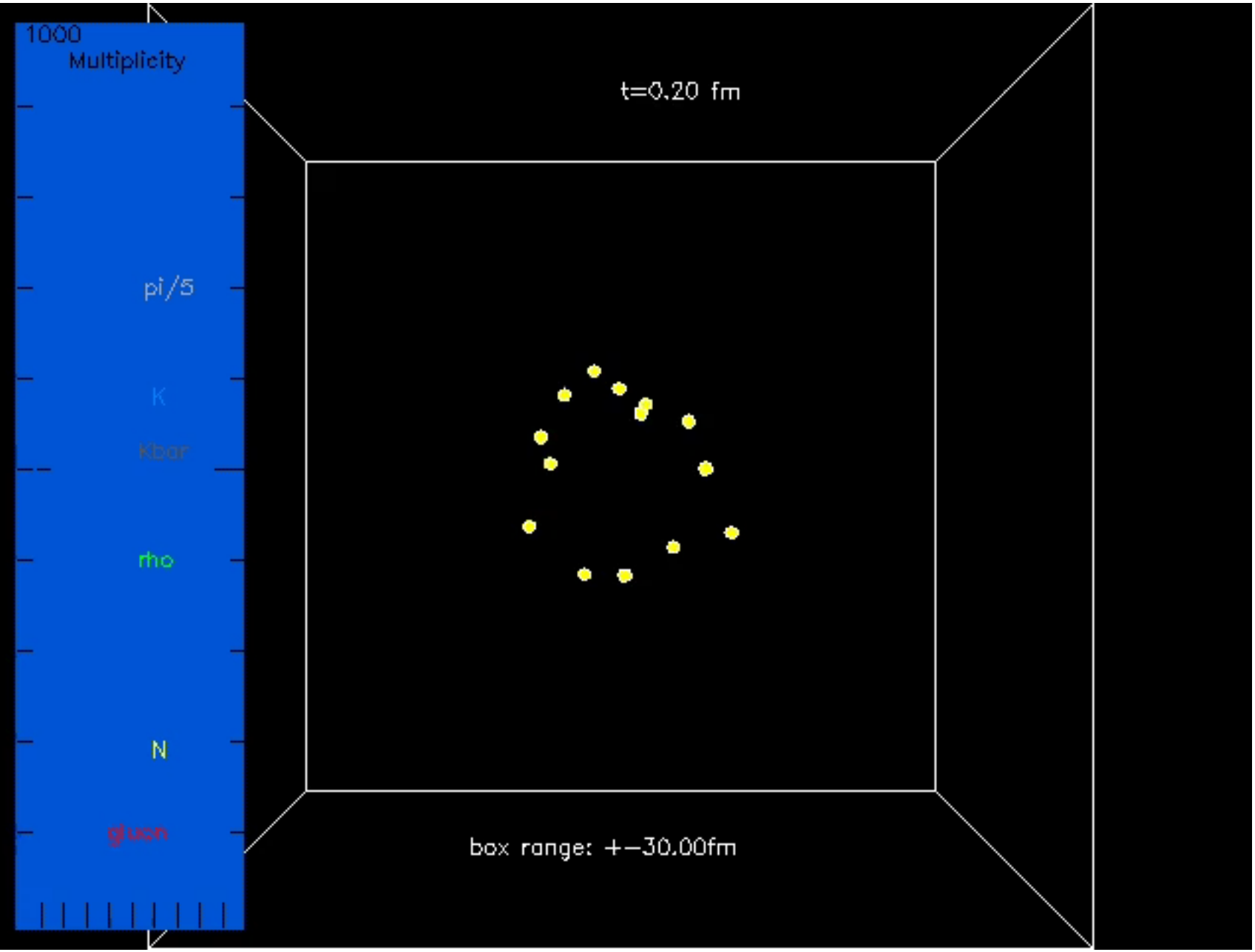

60fm-long box; shows only formed particles.

⊙

Beam axis

1st frame:
right after the primary collision, only spectator nucleons are formed.

At middle right:
a rho decays at 7.0 fm/c.

At lower right:
*a K*bar is produced at 16.6 fm/c & vanishes at 20.8fm/c.*

The same Au+Au event at 200AGeV from the Default AMPT model

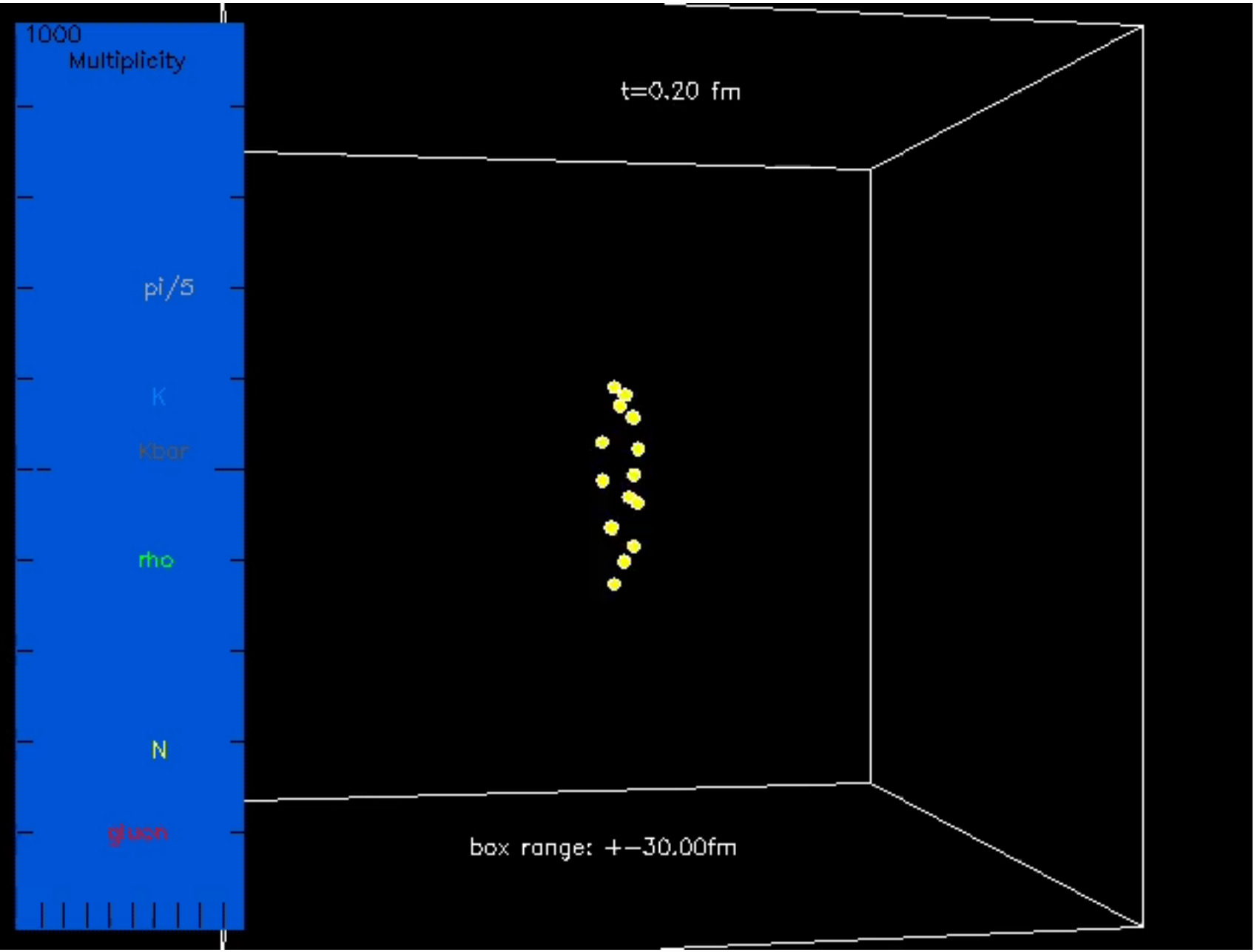

Side view:

Beam axes

Dynamics is time-dilated at large rapidities: for example, see hadronization of gluons

String Melting version of AMPT

If we use the Bjorken formula to estimate the initial energy density in AA collisions:

$$e_0 \sim \frac{dE_T/dy}{pR^2 t_0} \gg \frac{dE_T/dy}{150\,fm^3}$$

~ 2.5 SPS 6 RHIC 20 GeV/fm^3 LHC

Nuclear radius

Proper formation time, taken as *1 fm/c*

>>critical energy density for QCD phase transition:

$\varepsilon_c \sim$ O(1/2) GeV/fm^3

➔At high-enough energies,

hadronic matter such as strings cannot exist at early times,

they should be represented by a dense partonic matter

➔ the string melting version of AMPT ZWL & Ko, PRC (2002)

String Melting version of AMPT

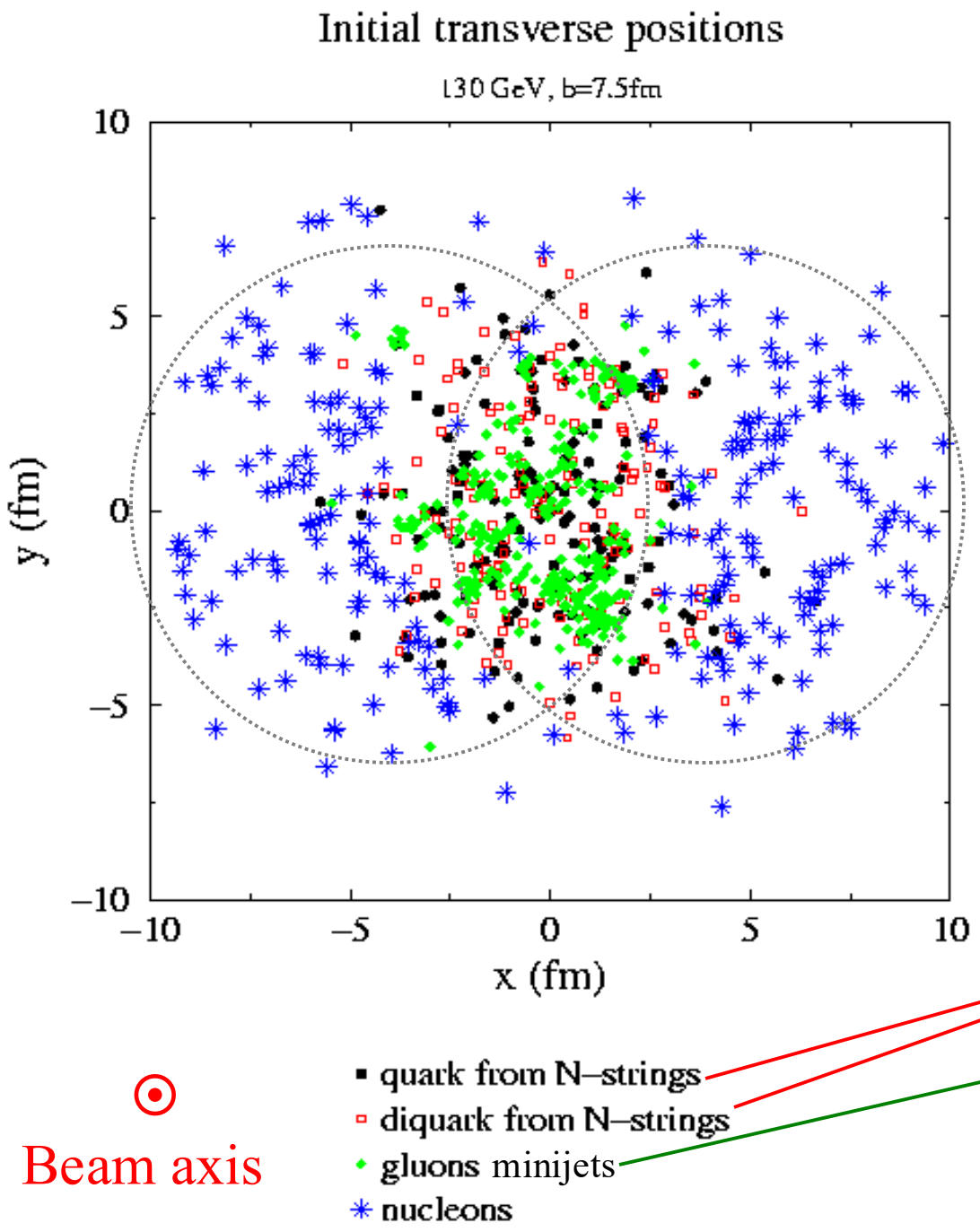

Soft strings are
in the high density overlap area,
but in the default model
they are not in the parton cascade.

With String Melting:
we convert strings into partonic matter.

Initial condition:
soft (strings) & *hard (minijets)*

Structure of AMPT v2.xx (String Melting version)

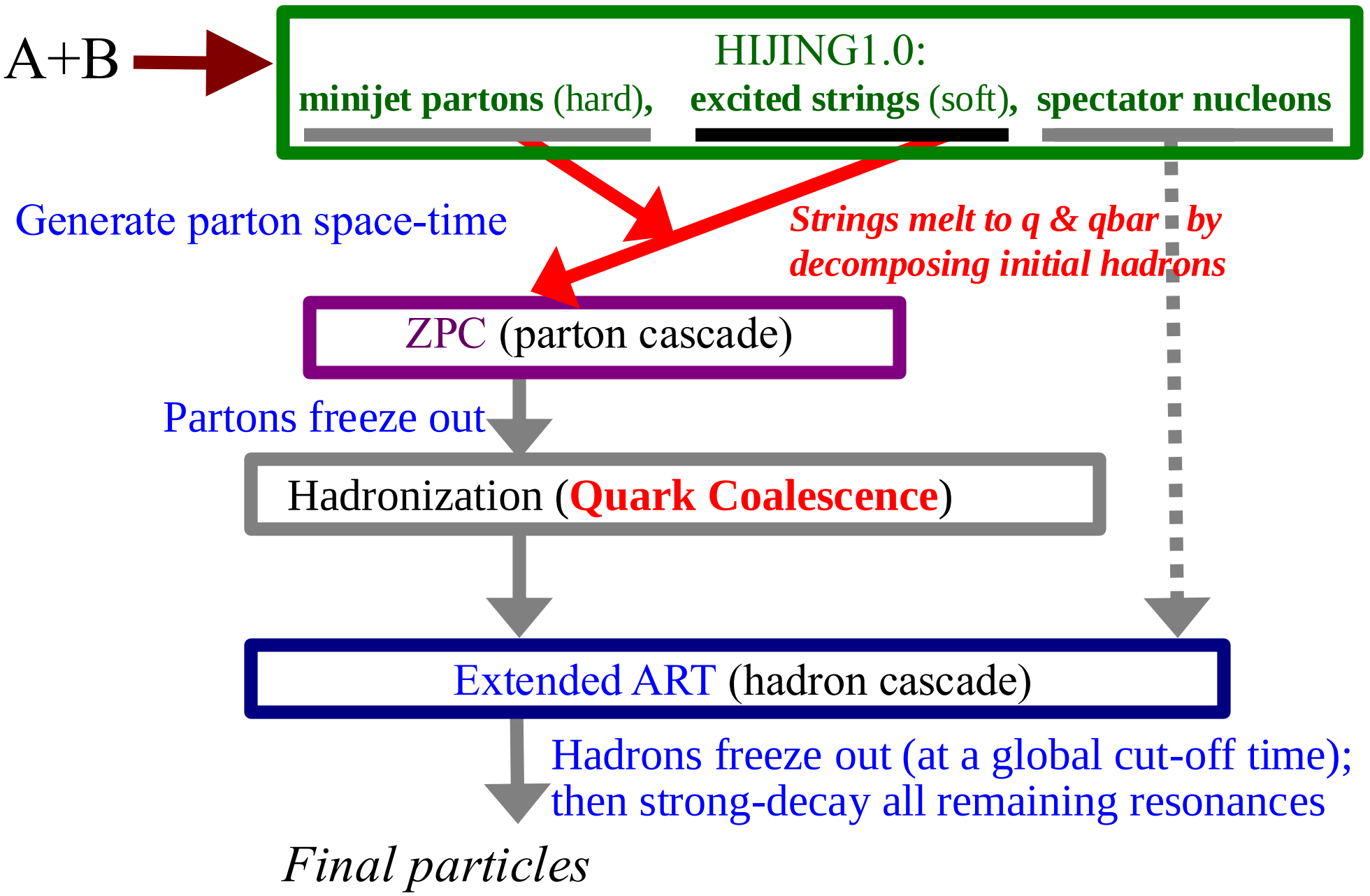

The same Au+Au event at 200AGeV from the String Melting AMPT

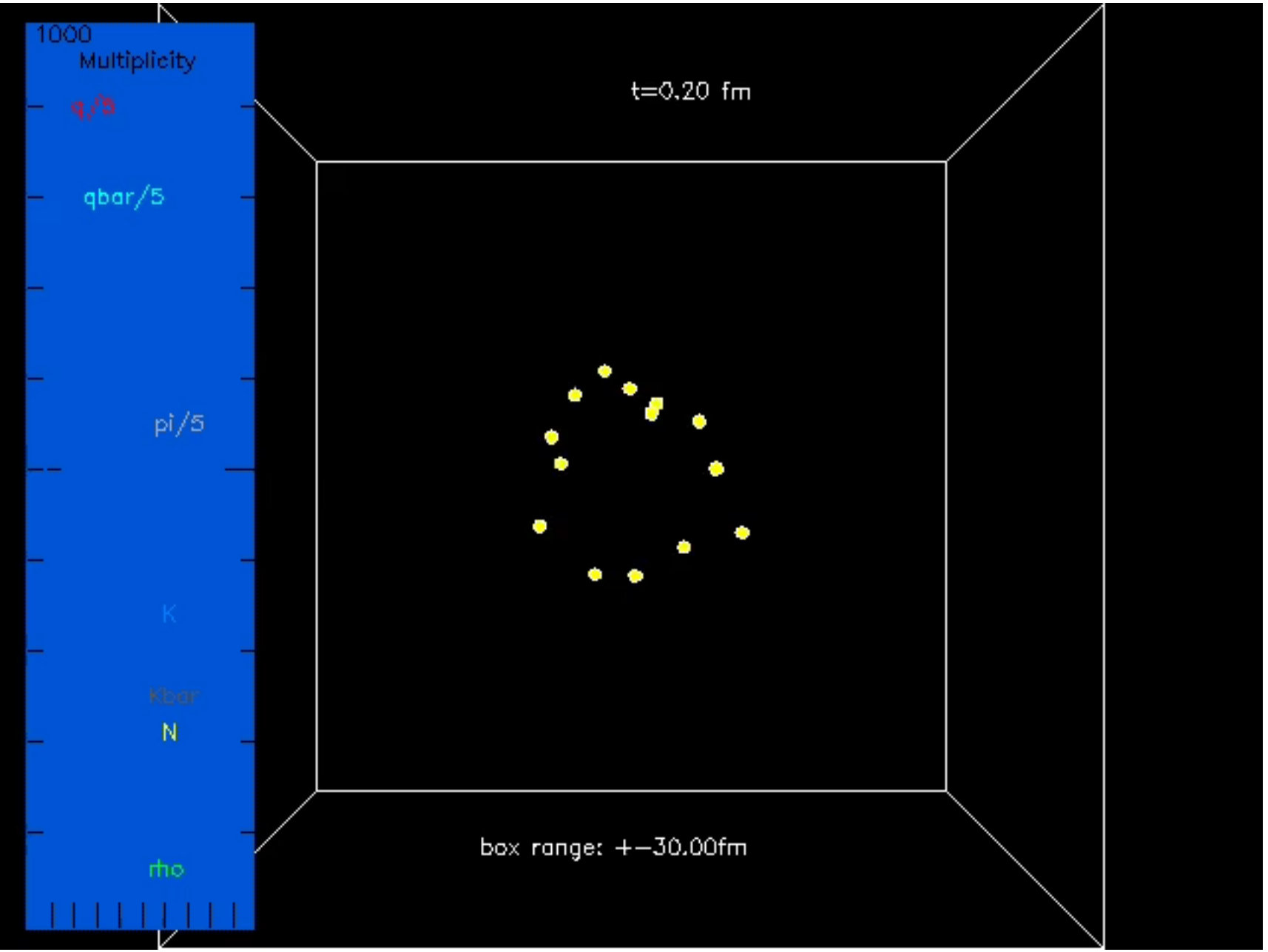

σ_p=3mb

⊙

Beam axis

The same Au+Au event at 200AGeV from the String Melting AMPT

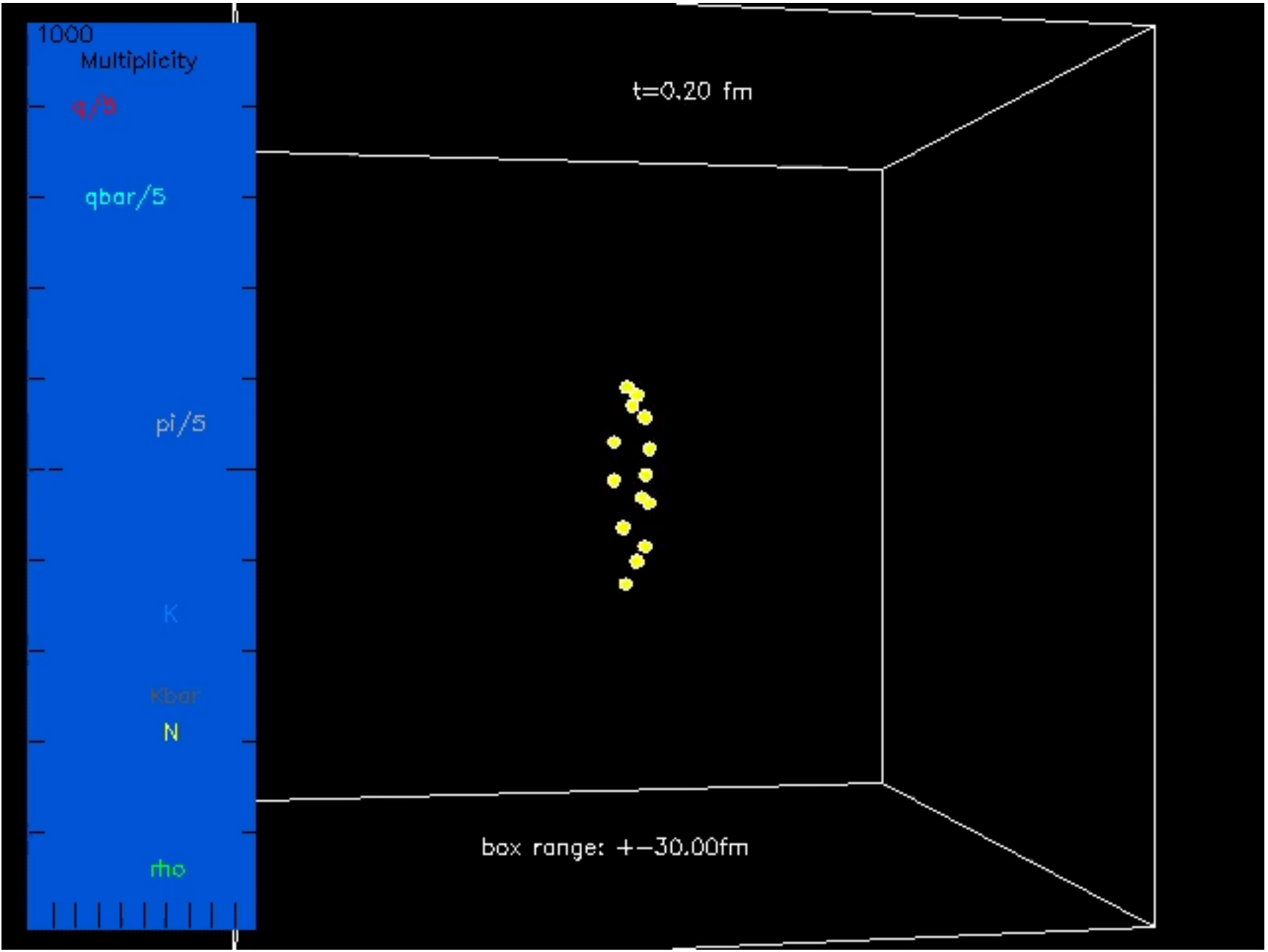

Side view:

Beam axes

Middle region (near mid-rapidity): coalescence of q (red) and qbar (cyan) occurs earlier

Compare the same event:

Default AMPT vs String Melting AMPT

at t=5 fm/c:

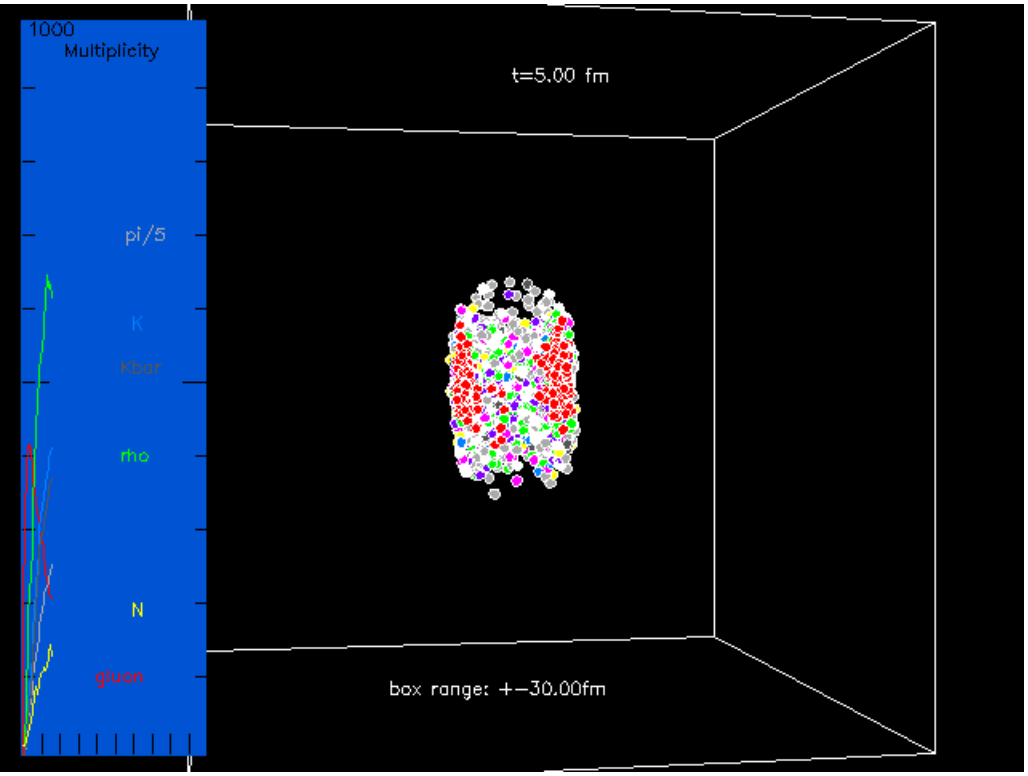

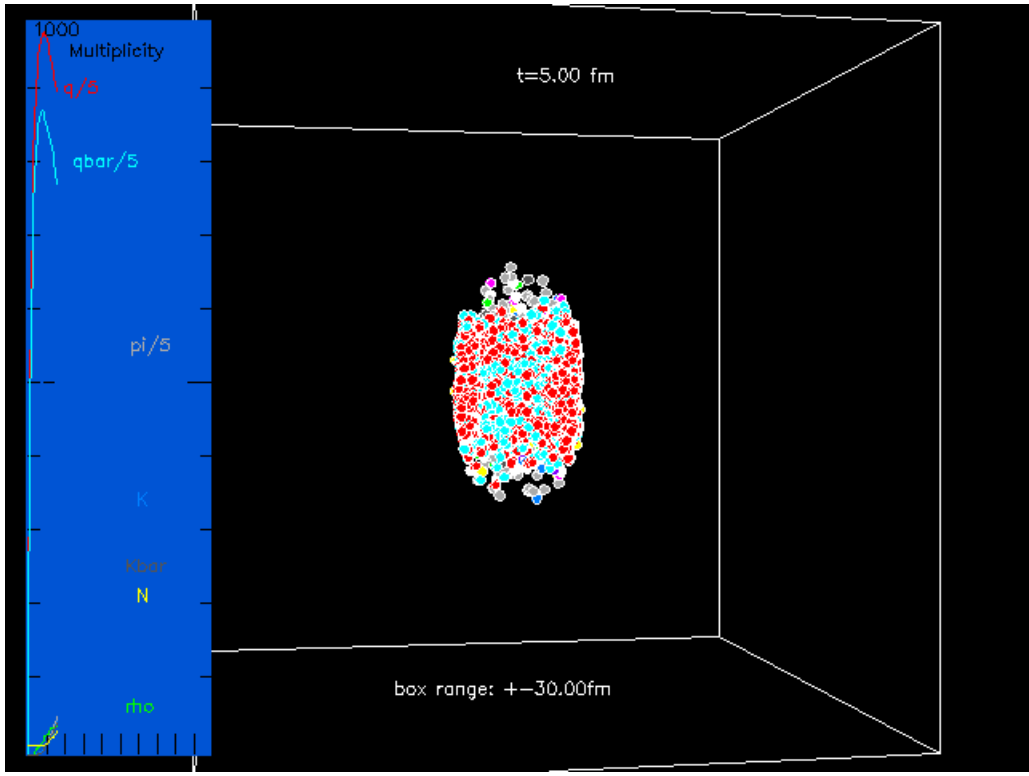

Beam axes

With String Melting:

many more partons,

parton stage is more important

& hadron stage starts much later

Individual components of AMPT

HIJING1.0	Two component model (*soft strings* + *hard minijets*)
ZPC	parton cascade (*elastic collisions only*)
Hadronization	Lund string fragmentation (*Default AMPT*) or Quark coalescence (*String Melting AMPT*)
Extended ART	Hadron cascade, including secondary interactions for p r w h K K^* f n p D $N^*(1440)$ $N^*(1535)$ L S X W *deuteron*

All other particles with PYTHIA flavor codes have no secondary interactions, but they will be produced (*from HIJING or quark coalescence*), e.g. D D_s J/Ψ B Υ.

Each hadron has an explicit isospin/charge.

Individual component 1: initial condition from String Melting

String Melting converts strings into quarks and antiquarks:

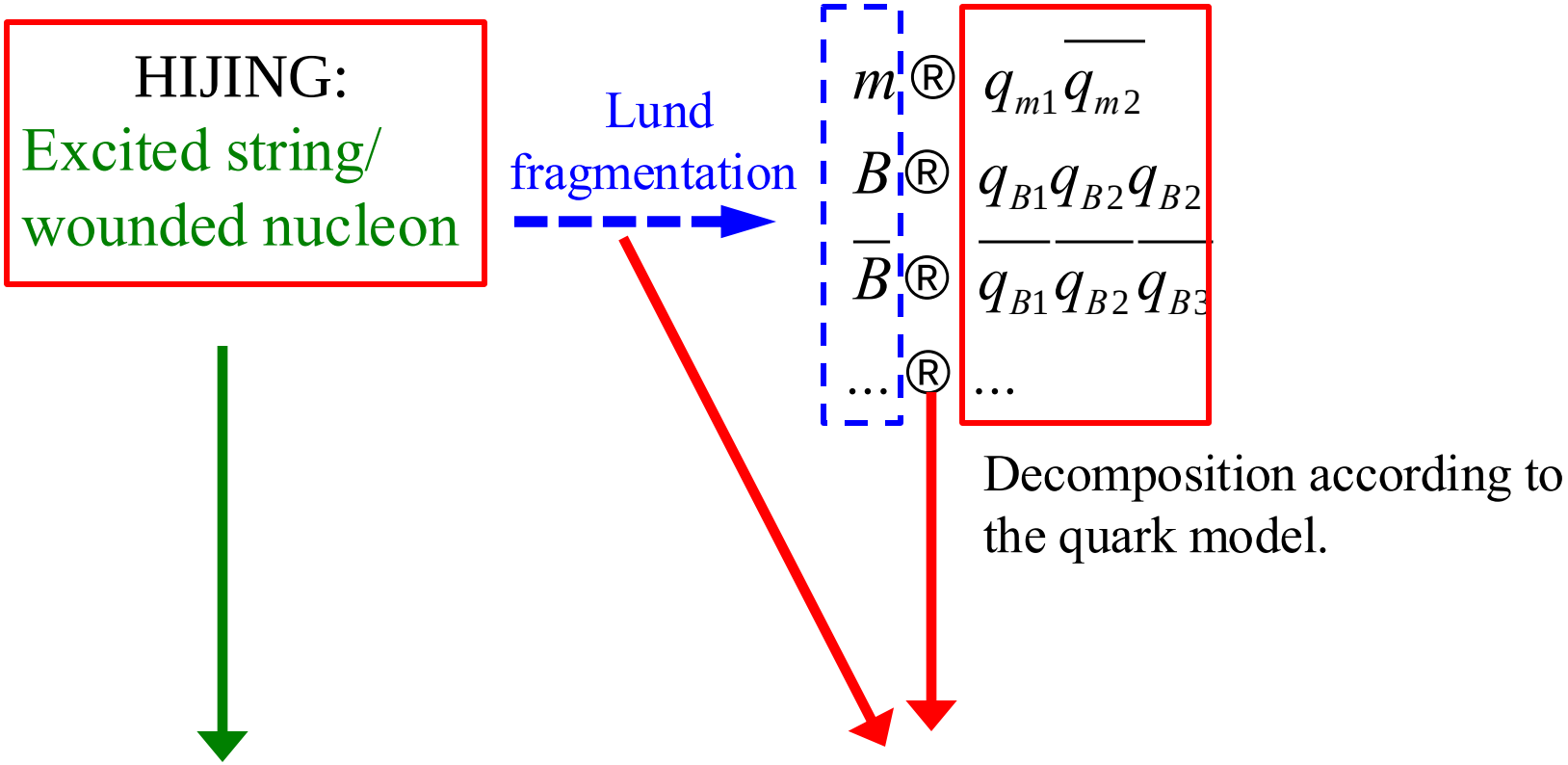

Include fluctuations
of nucleon positions
from Monte Carlo Glauber

String Melting introduces additional fluctuations to the initial condition:

- through random nature of minijet production, string fragmentation and decomposition
- leads to longitudinal correlation of partons from the same string (~flux tube)

Individual component 2: parton cascade

Currently, ZPC solves the Boltzmann equation for 2-body scatterings:

$$\partial_t f + \frac{\partial \boldsymbol{x}}{\partial t} \cdot \nabla_x f = C[\lfloor M^2 \rfloor f_1 f_2] \propto \sigma f_1 f_2$$

- $gg \circledR gg$ cross section in leading-order pQCD is used

$$\frac{d\sigma_{gg}}{dt} = \frac{9\pi\alpha_s^2}{2s^2}\left(3 - \frac{ut}{s^2} - \frac{us}{t^2} - \frac{st}{u^2}\right) \simeq \frac{9\pi\alpha_s^2}{2}\left(\frac{1}{t^2} + \frac{1}{u^2}\right) \simeq \frac{9\pi\alpha_s^2}{2t^2}$$

Bin Zhang, Comp Phys Comm (1998);
ZWL, Ko, Li, Zhang & Pal, PRC (2005)

- σ is divergent for massless g, so a Debye screening mass μ is applied:

$$\frac{d\sigma}{dt} = \frac{9\pi\alpha_s^2}{2}\frac{1+a}{(t-\mu^2)^2}$$

$a \equiv \frac{\mu^2}{s}$ is added to obtain an s-independent cross section: $\sigma = \frac{9\pi\alpha_s^2}{2\mu^2}$

Individual component 2: parton cascade

Currently, ZPC solves the Boltzmann equation for 2-body scatterings:

$$\partial_t f + \frac{\partial \boldsymbol{x}}{\partial t} \cdot \nabla_x f = C[\lfloor M^2 \rfloor f_1 f_2] \propto \sigma f_1 f_2$$

Naively, the cascade solution using geometric cross sections is only accurate in the dilute limit when the opacity parameter χ is small:

$$\chi \equiv \frac{r}{\lambda} = \frac{\sigma^{3/2} n}{\sqrt{\pi}} \quad < 1,$$

Zhang, Gyulassy & Pang, PRC (1998)

i.e., when the range of particle interaction r < mean free path λ

$$r \equiv \sqrt{\frac{\sigma}{\pi}} \qquad \lambda = \frac{1}{\sigma n}$$

At at large densities n and/or cross sections σ,
ZPC/MPC cascade solution of the relativistic Boltzmann equation (RBE) has been well known to suffer from causality violation.

Zhang, Comp Phys Comm (1998);
Monlar & Gyulassy, PRC (2000); Cheng et al., PRC (2002); …

Individual component 2: parton cascade

Particle subdivision (or the test particle method) reduces/removes causality violation:

Pang, CU-TP-815 (1996)
Gyulassy, Zhang, Pang, PRC (1998)

$$\partial_t f + \frac{\partial \boldsymbol{x}}{\partial t} \cdot \nabla_x f = C[\lfloor M^2 \rfloor f_1 f_2] \propto \sigma f_1 f_2$$

This is because the above Boltzmann equation is invariant under transformation:

$f \longrightarrow f * l$ and $\sigma \longrightarrow \frac{\sigma}{l}$ ($\frac{\mathrm{d}\sigma}{dt} \longrightarrow \frac{\mathrm{d}\sigma}{dt}/l$ *to be exact*)

Xin-Li Zhao, Ma, Ma & ZWL, PRC (2020)

which reduces the opacity χ to approach the dilute limit:

$$\chi \equiv \frac{\sigma^{3/2} n}{\sqrt{\pi}} \longrightarrow \frac{\chi}{\sqrt{l}}$$

l: subdivision factor

However, subdivision method is very CPU-consuming;
more importantly, it drastically changes event-by-event fluctuations & correlations.

→ much better to have an accurate parton cascade (*without using subdivision*)

Individual component 3: hadronization in Default AMPT

HIJING produces

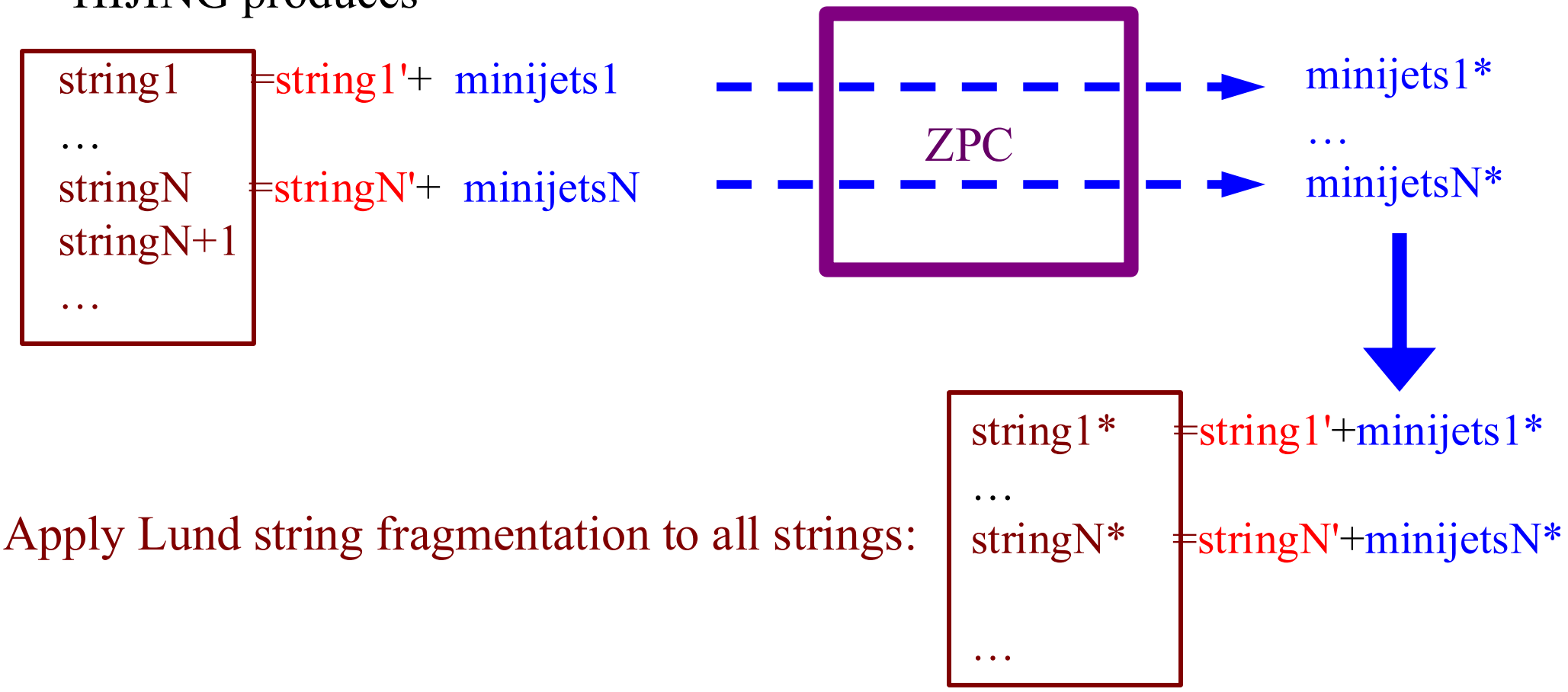

Apply Lund string fragmentation to all strings:

Minijet partons recombine with the original string':

to ensure success of string fragmentation,

e.g. to avoid fractional total charge for a string

Individual component 3: quark coalescence in String Melting

Original/old algorithm of quark coalescence:

ZWL & Ko, PRC (2002)

A parton finds the closest partner in space to form a hadron:

q_{m1} finds the closest $\bar{q}_2$ → forms a meson

q_{B1} finds the closest q_2, q_3 → forms a baryon

Then determine flavor of the formed hadron,

for example:

$\bar{u}d$: forms ρ^- if invariant mass is closer to m_ρ

forms r^- if invariant mass is closer to m_r

$\bar{u}u$: lowest masses form ρ^0, with $\#\rho^0 = (\#\rho^+ + \#\rho^-)/2$

then form r^0, with $\#r^0 = (\#r^+ + \#r^-)/2$

then form w and h with equal probability

Individual component 3: quark coalescence in String Melting

New algorithm of quark coalescence:

He & ZWL, PRC (2017)

A parton finds the closest partner in space to form a hadron:

q_1 finds the closest $\overline{q}_2$ → possible meson (M) formation

& finds the closest q_2, q_3 → possible baryon (B) formation

Then formation of M or B is decided by comparing distances between the 2 or 3 coalescing partons for the two possible formations.

This gives quark the freedom to form either M or B; this is more physical and also leads to better antiB/B ratios:

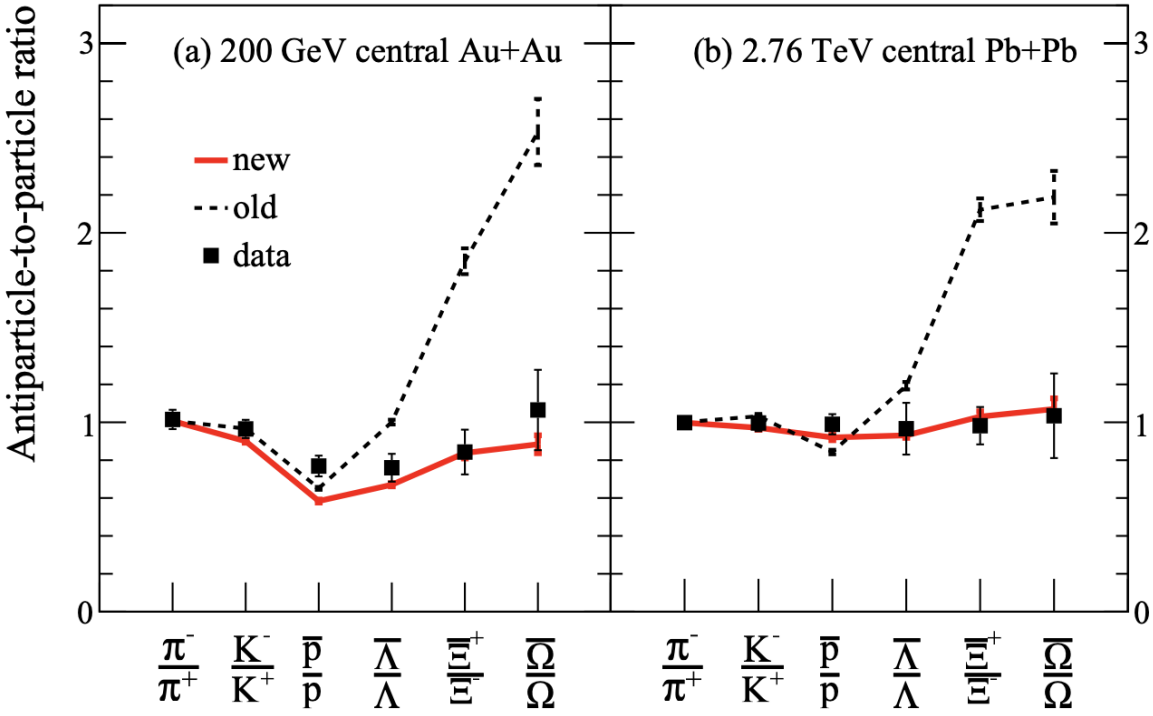

Individual component 4: hadron cascade

Based on the ART model	Li & Ko, PRC 52 (1995)
$\overline{K}$ interactions added	Song, Li & Ko, NPA 646 (1999)
$N\overline{N}$ annhilation, K^0 productions	Zhang et al, PRC 61 (2000)
$B\overline{B}$ « mesons, explicit K^*	ZWL et al, PRC 64 (2001), NPA 698 (2002)
η interactions	ZWL & Ko, PRC 65 (2002)
φ interactions	Pal, Ko & ZWL, NPA 707 (2002)
Multi-strange interactions ($\Lambda\ \Sigma\ \Xi\ \Omega$)	Pal, Ko & ZWL, NPA 730 (2004)
Deuteron interactions	Oh, ZWL & Ko, PRC 80 (2009), NPA 834 (2010)

Individual component 4: hadron cascade

Meson-Meson channels:

SU(2): $\pi\pi \leftrightarrow \rho, \pi\pi$ direct

$\pi\pi \leftrightarrow \rho\rho$

elastic scatterings with 20mb

η meson scatterings

With strangeness: $(\pi/\eta)(\pi/\eta) \leftrightarrow K\bar{K}$

$(\rho/\omega)(\rho/\omega) \leftrightarrow K\bar{K}$

$(\pi/\eta)(\rho/\omega) \leftrightarrow K^*\bar{K}$ or $\bar{K}^*K, \cdots$

$(K/K^*)(\rho\omega\eta)$ elastic with 10mb

$\phi\bar{K} \leftrightarrow (\pi/\rho)(K/K^*), \cdots$

Individual component 4: hadron cascade

Meson-Baryon channels:

$\pi N \leftrightarrow \Delta/N^*(1440)/N^*(1535);\ \eta N \leftrightarrow N^*(1535)$

$\pi N \leftrightarrow (\pi/\rho/\omega)\Delta$

$\bar{K}N \leftrightarrow \pi(\Lambda/\Sigma);\ \bar{K}(\Lambda/\Sigma) \leftrightarrow \pi\Xi;\ \bar{K}\Xi \leftrightarrow \pi\Omega$

$(\pi/\rho/\omega/\eta)(N/\Delta/N^*) \leftrightarrow K(\Lambda/\Sigma)$

$(\pi/\rho/\omega)(N/\Delta/N^*) \rightarrow N\bar{K}K$

$(\pi/\rho/\omega/K/K^*)(N/\Delta/N^*)$ elastic

ϕN channels, $\cdots$

Baryon-Baryon channels:

$B_1B_2 \leftrightarrow B_3B_4,\ B \equiv N/\Delta/N^*$

$NN \rightarrow \Delta\Delta(\pi/\rho), \cdots,\ B_1B_2 \rightarrow NK(\Lambda/\Sigma)$

Baryon-antiBaryon channels:

$B\bar{B} \leftrightarrow MM;\quad B \equiv N/\Delta/N^*,\ M \equiv \pi/\rho/\omega$

e.g. $p\bar{p} \leftrightarrow \rho\omega\ (\sim 5\pi);\quad \leftrightarrow \omega\omega\ (\sim 6\pi)$

The AMPT source code has been online since ~ April 2004:

https://myweb.ecu.edu/linz/ampt/

AMPT source codes

(updated December 25, 2018):

A Multi-Phase Transport (AMPT) model is a Monte Carlo transport model for nuclear collisions at relativistic energies.
Each of the following versions contains:
the source codes, an example input file, a Makefile, a readme, a required subdirectory for storing output files, and a script to run the code.

1. ampt-v1.11-v2.11.tgz (11/2004)
2. ampt-v1.21-v2.21.tgz (10/2008)
3. *Other older versions inbetween*
4. ampt-v1.26t5-v2.26t5.zip (4/2015)
5. ampt-v1.26t7-v2.26t7.zip (10/2016)
6. ampt-v1.26t7b-v2.26t7b.zip (5/2018)
7. ampt-v1.26t9-v2.26t9.zip (9/2018)
8. ampt-v1.26t9b-v2.26t9b.zip (12/2018)

String Melting AMPT since 4/2015 can reasonably describe bulk matter at high energies.

This readme file lists the main changes up to version v1.26t9b-v2.26t9b ("t" means a version under test):

```
AMPT Users' Guide

%%%%%%%%%%%%%%%%%%%%%%%%%%%%%%%%%%%%%%%%%%%%%%%%%%%%%%%%%%%%%%%%%%%%%%%
12/2018 test version v1.26t9b/v2.26t9b:
     * Fixed bugs that can cause segmentation fault (especially for default
       AMPT at high energies):
```

Selected results: particle yields

Particle yields
from AGS to
RHIC energies
from Default AMPT:

ZWL et al. PRC 72 (2005)

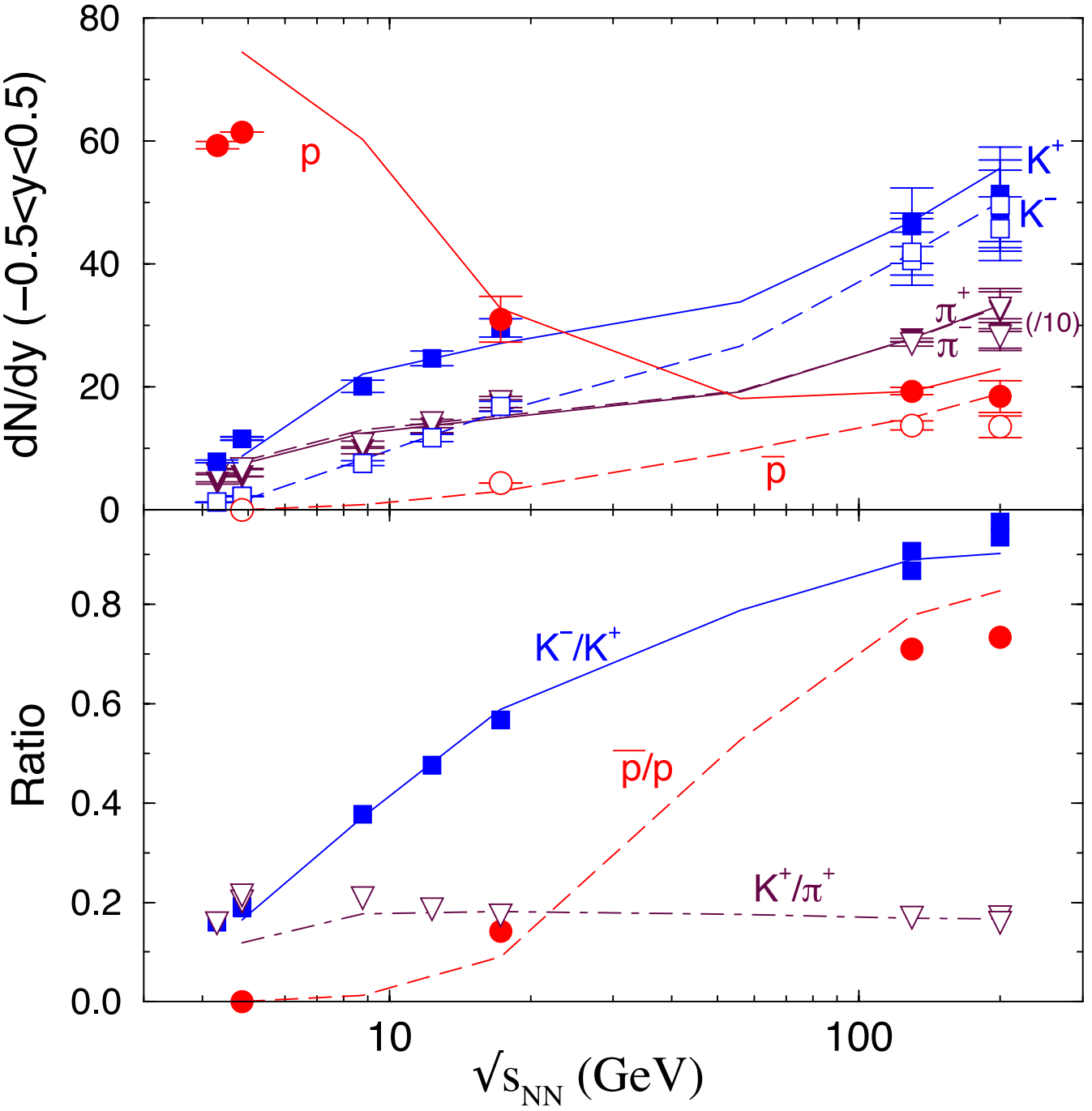

Selected results: spectra

FSI
=*Final State Interactions:*

lead to
more transverse flow.

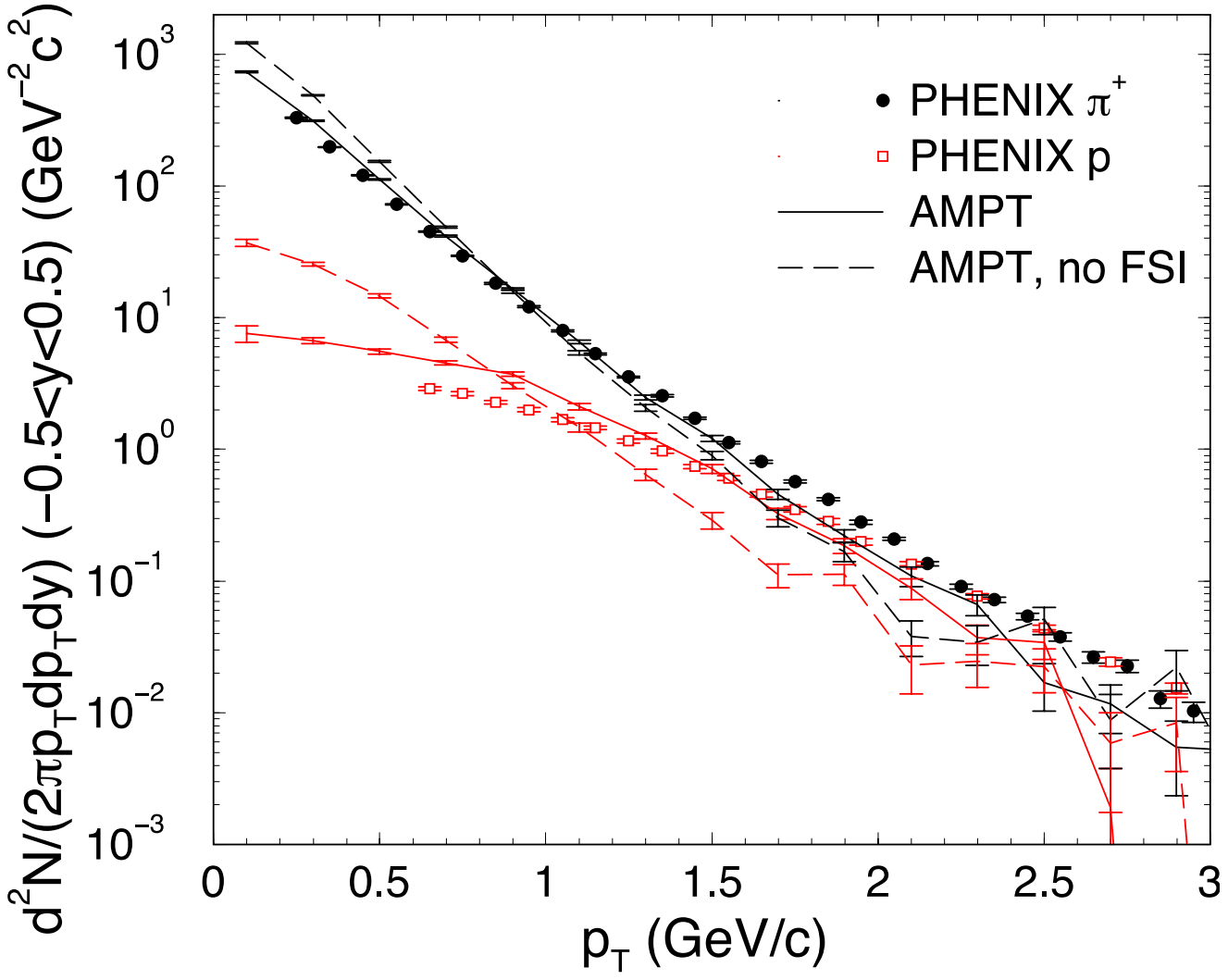

Selected results: v2

Elliptic flow v_2 at RHIC
Au+Au collisions@200 AGeV

String Melting AMPT:
if strings "melt" to partons, partonic interactions are strong enough to reproduce v_2

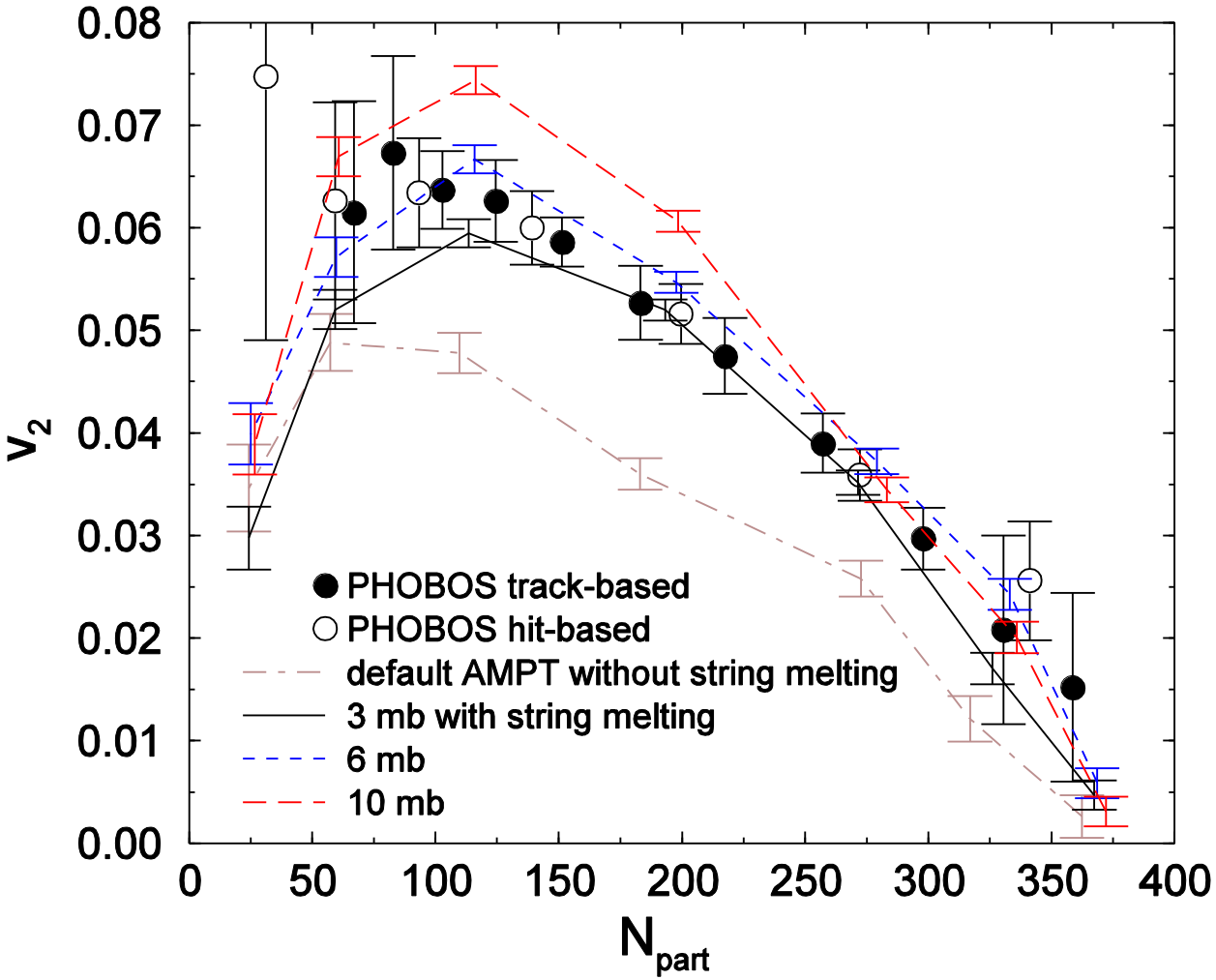

ZWL & Ko, PRC 65 (2002);
ZWL et al. PRC 72 (2005)

Selected results: HBT

Two-particle Bose-Einstein correlations in Hanbury Brown-Twiss interferometry

A transport model is needed to describe the non-equilibrium kinetic freeze-out process:

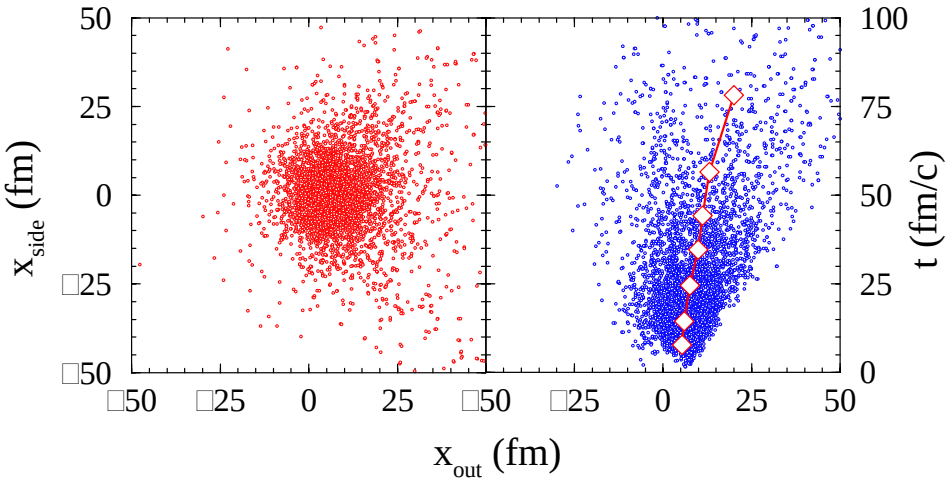

ZWL, Ko & Pal, PRL 79 (2002)

Model can roughly reproduce the RHIC HBT radius values

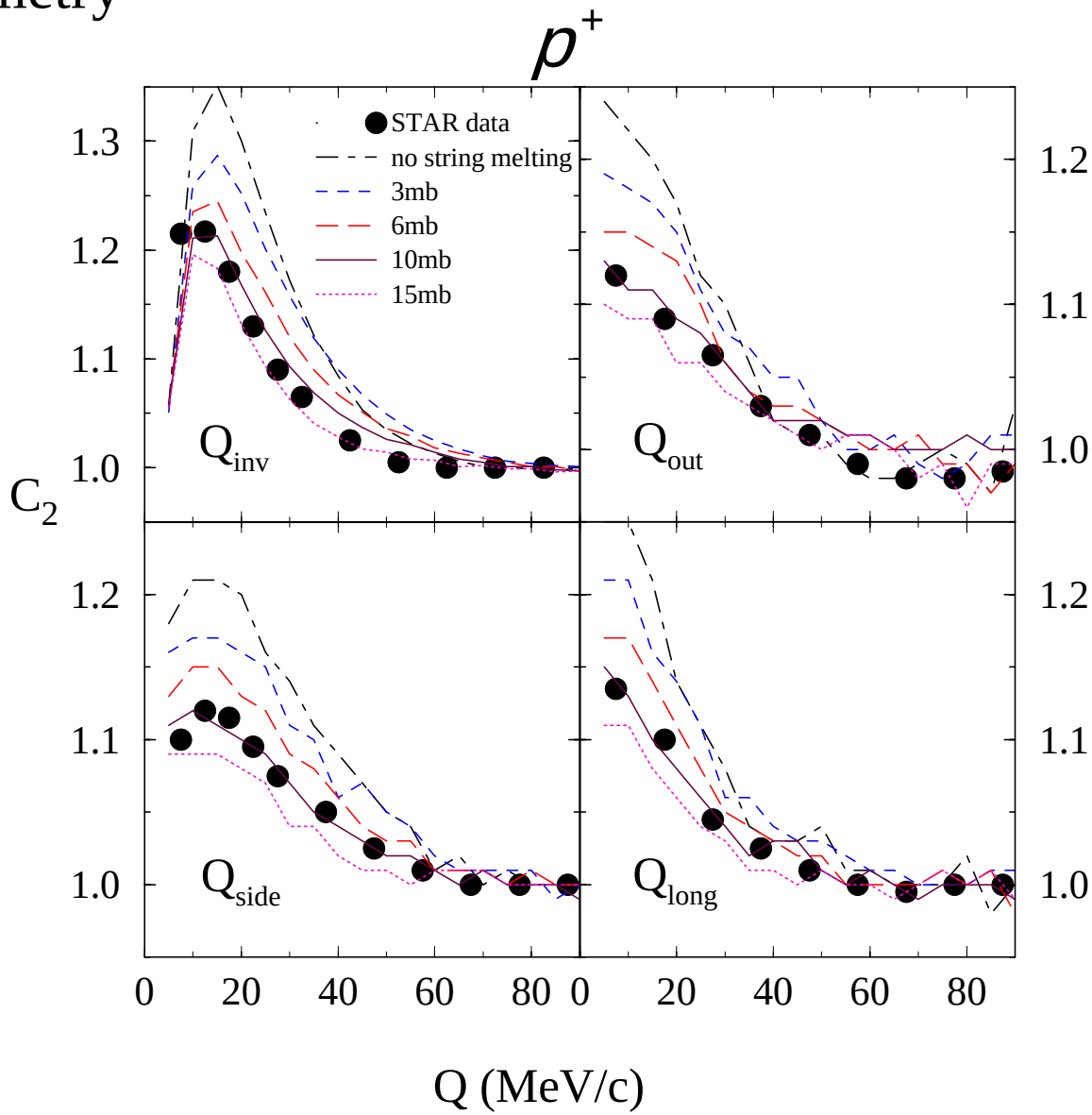

Selected results: improved String Melting model

The string melting AMPT model can reasonably reproduce

low-pT π & K data on *dN/dy*, p_T–spectra & *v2*

in central (0-5%) and mid-central (20-30%)

200AGeV Au+Au collisions (RHIC) and 2760AGeV Pb+Pb collisions (LHC)

ZWL, PRC 90 (2014)

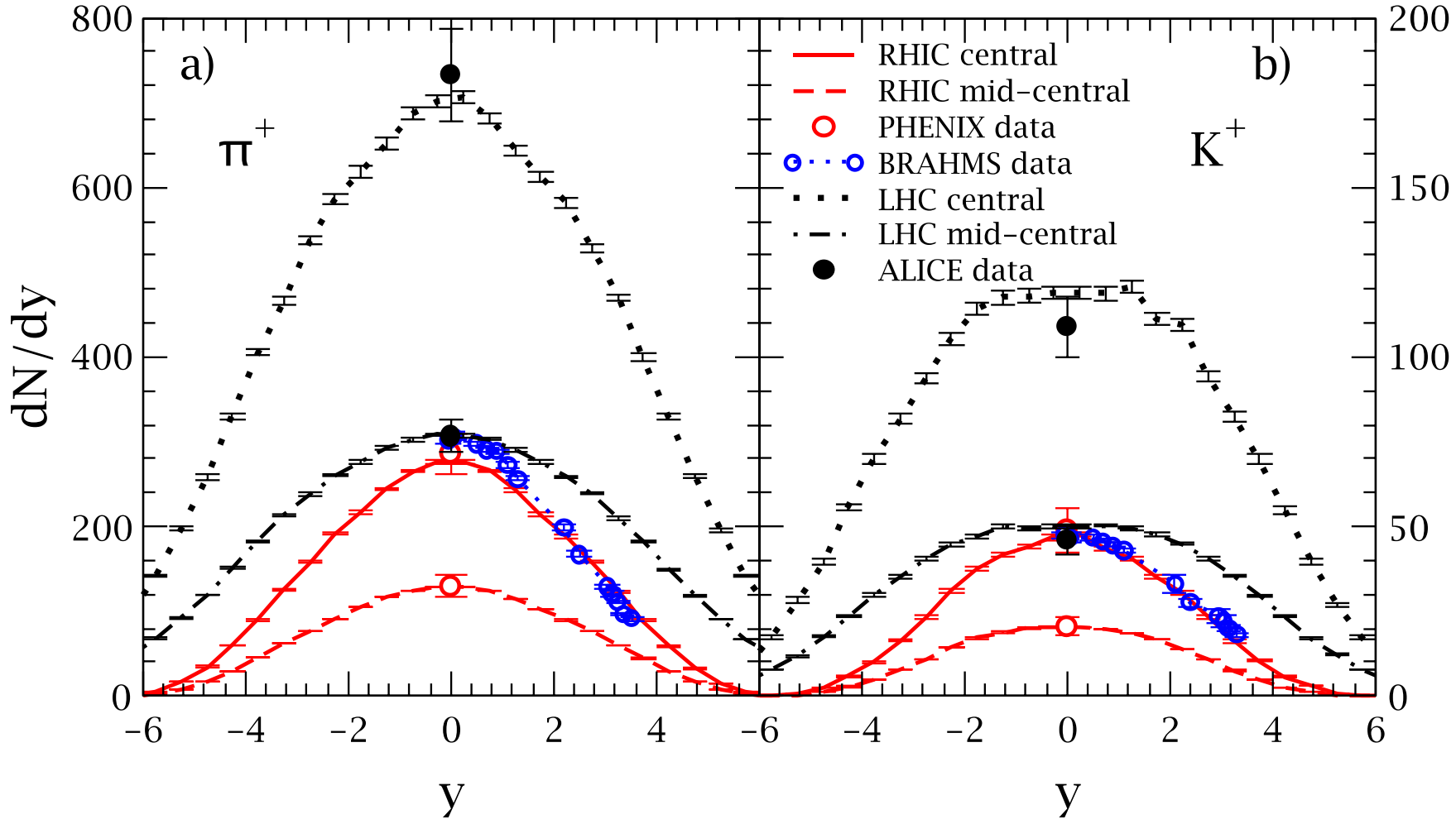

Selected results: improved String Melting model

p_T -spectra of π & K (in central collisions):

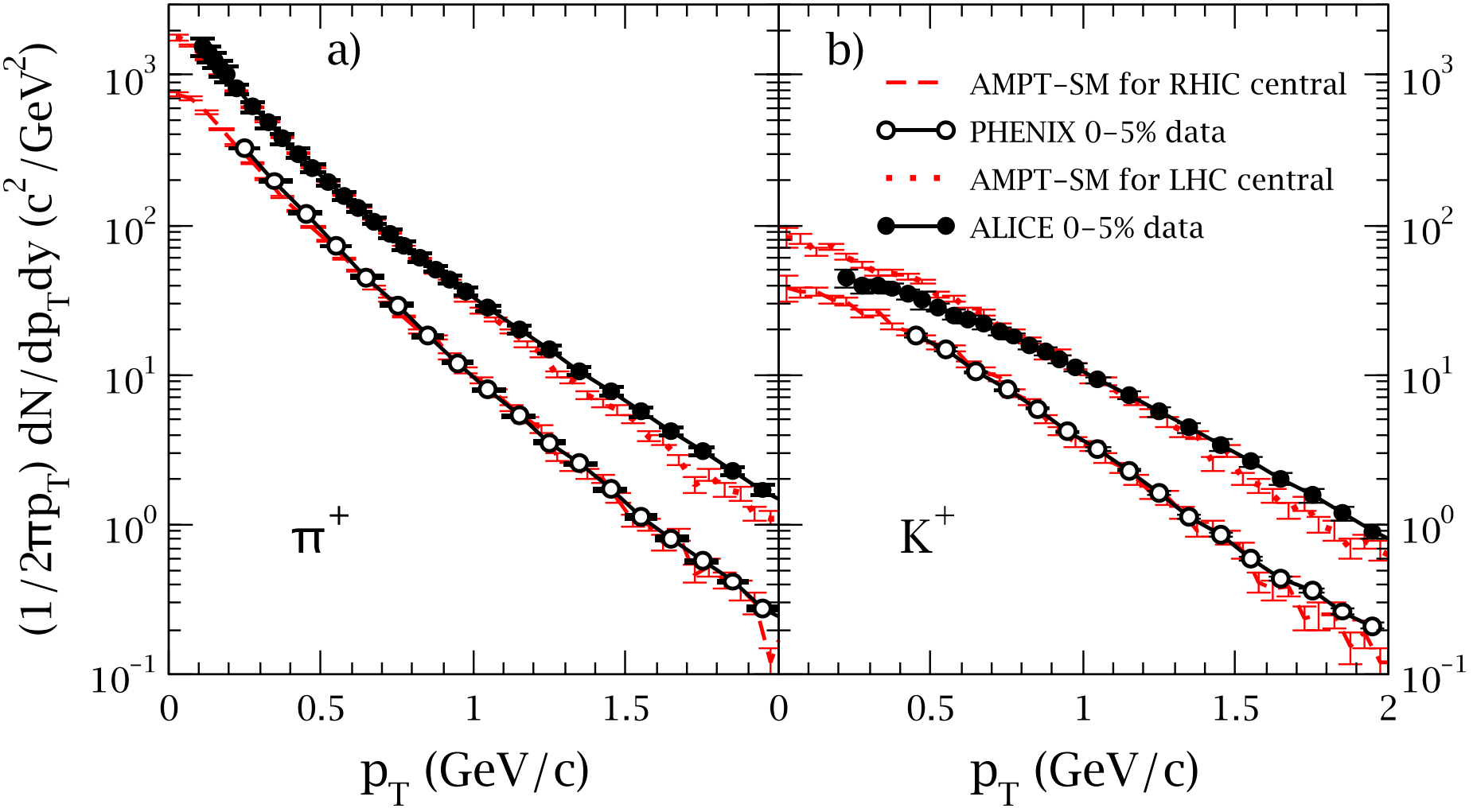

Selected results: improved String Melting model

v2 of π & K (in mid-central collisions):

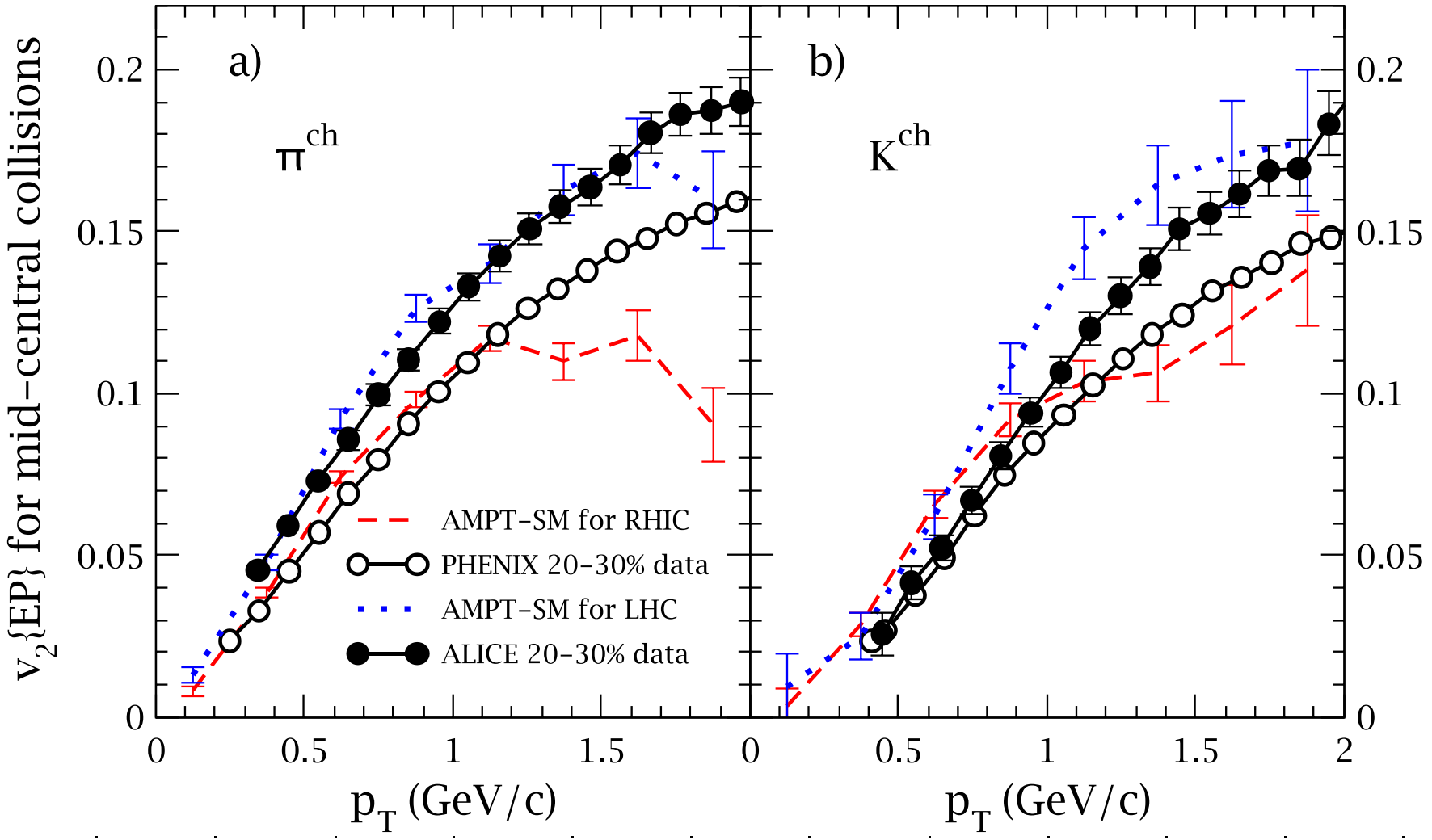

Selected results: predictions for 5ATeV Pb+Pb

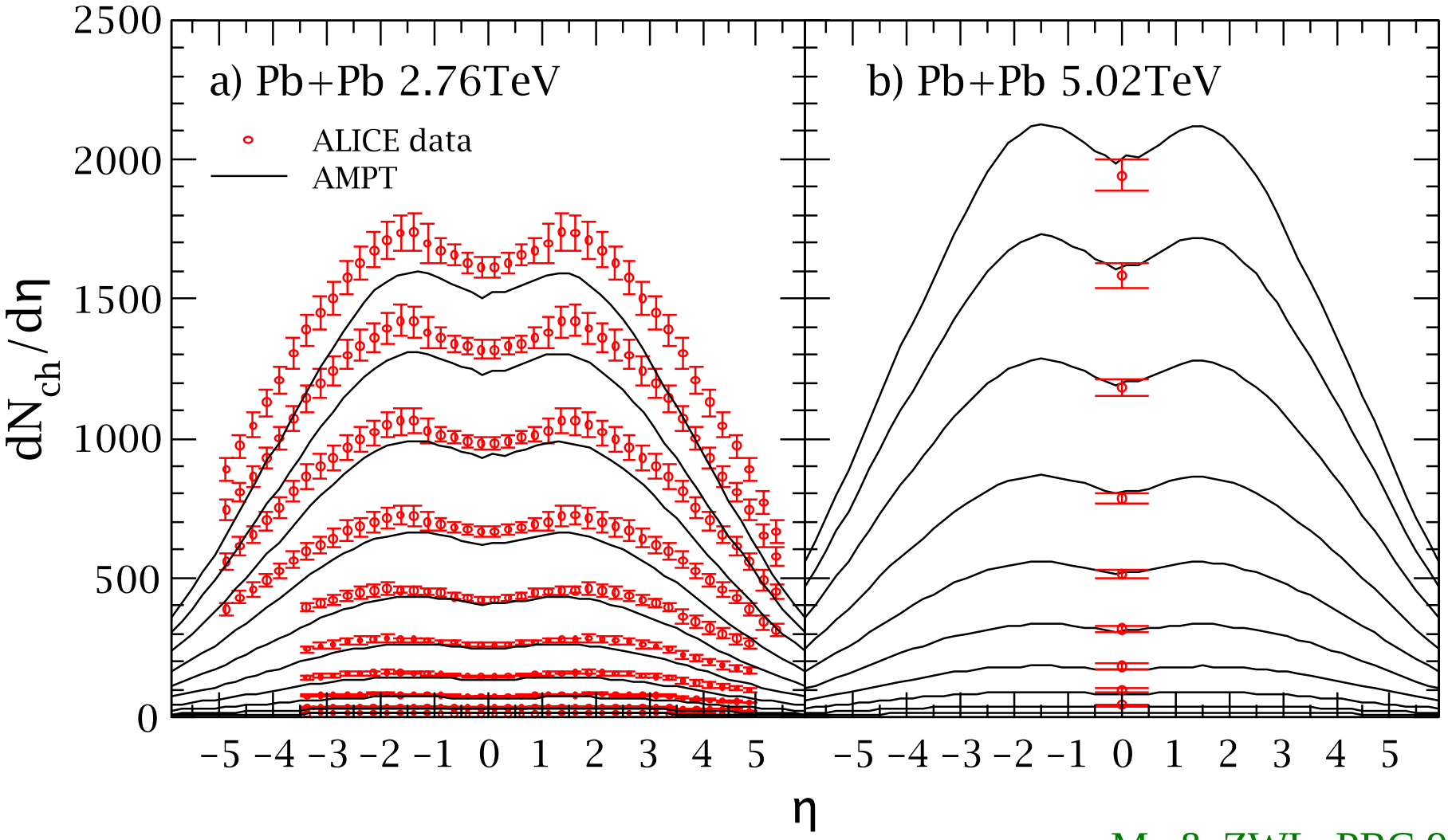

Ma & ZWL, PRC 93 (2016)

Although we had these dN/dη results before the announcement of the ALICE 5.02 TeV data, the paper was not posted before the data. Thus dN/dη values at η~0 are strictly speaking not predictions; the full dN/dη curves are still predictions.

Selected results: predictions for 5ATeV Pb+Pb

Charged particle flows v_2, v_3, v_4

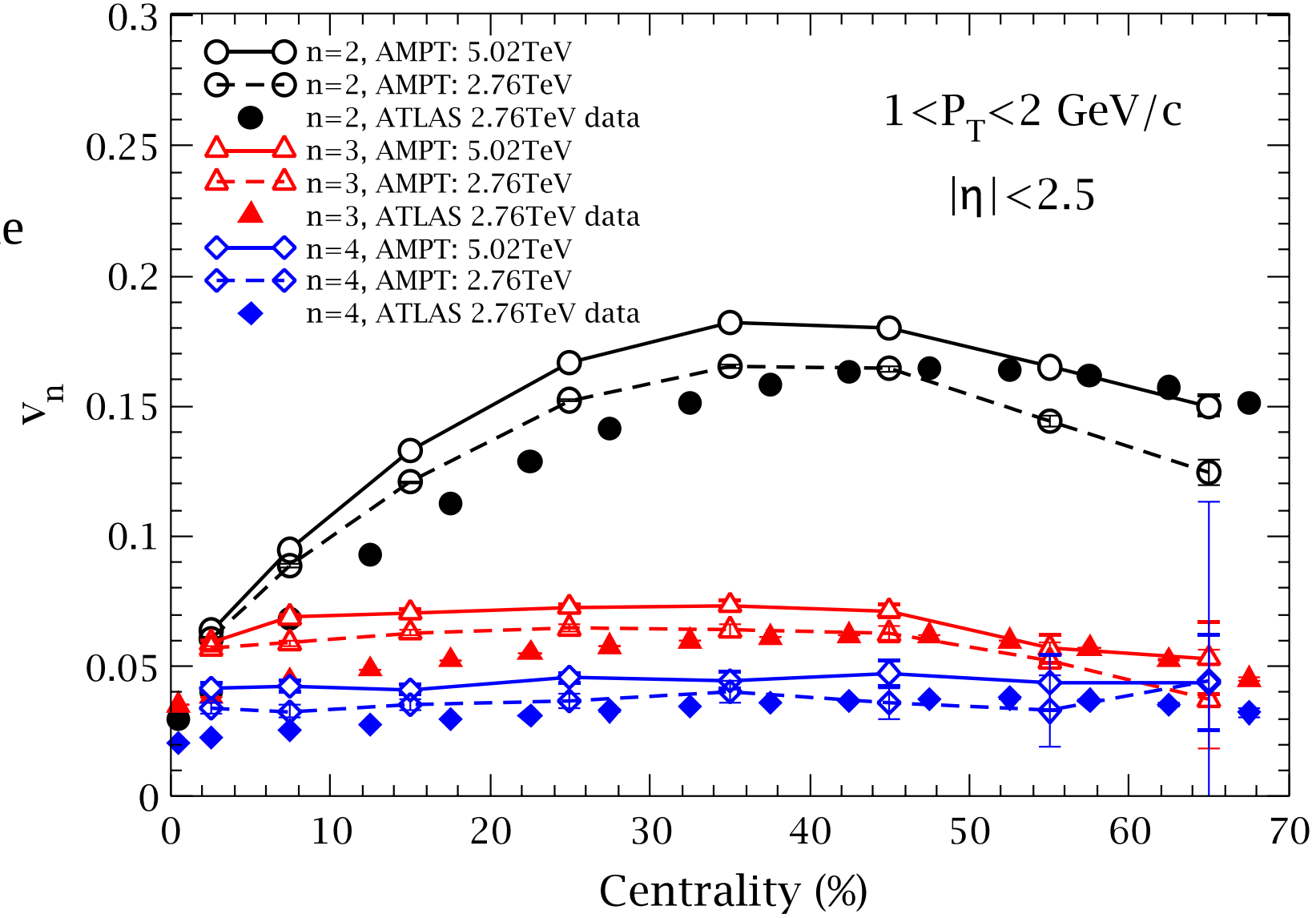

Selected results: predictions for 5ATeV Pb+Pb

Charged particle flows v_2, v_3, v_4

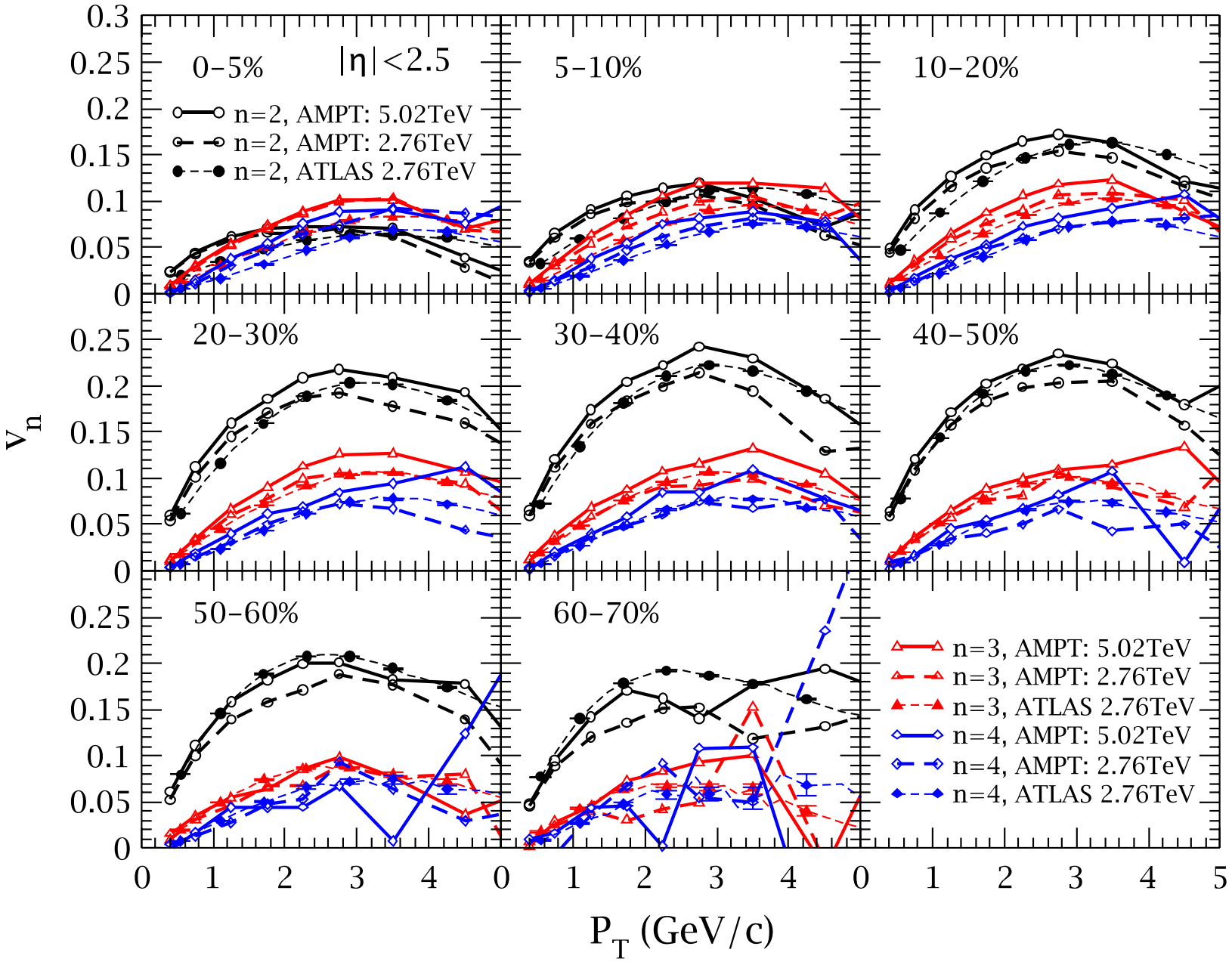

Selected results: predictions for 5ATeV Pb+Pb

Charged particle $v_2(\eta)$

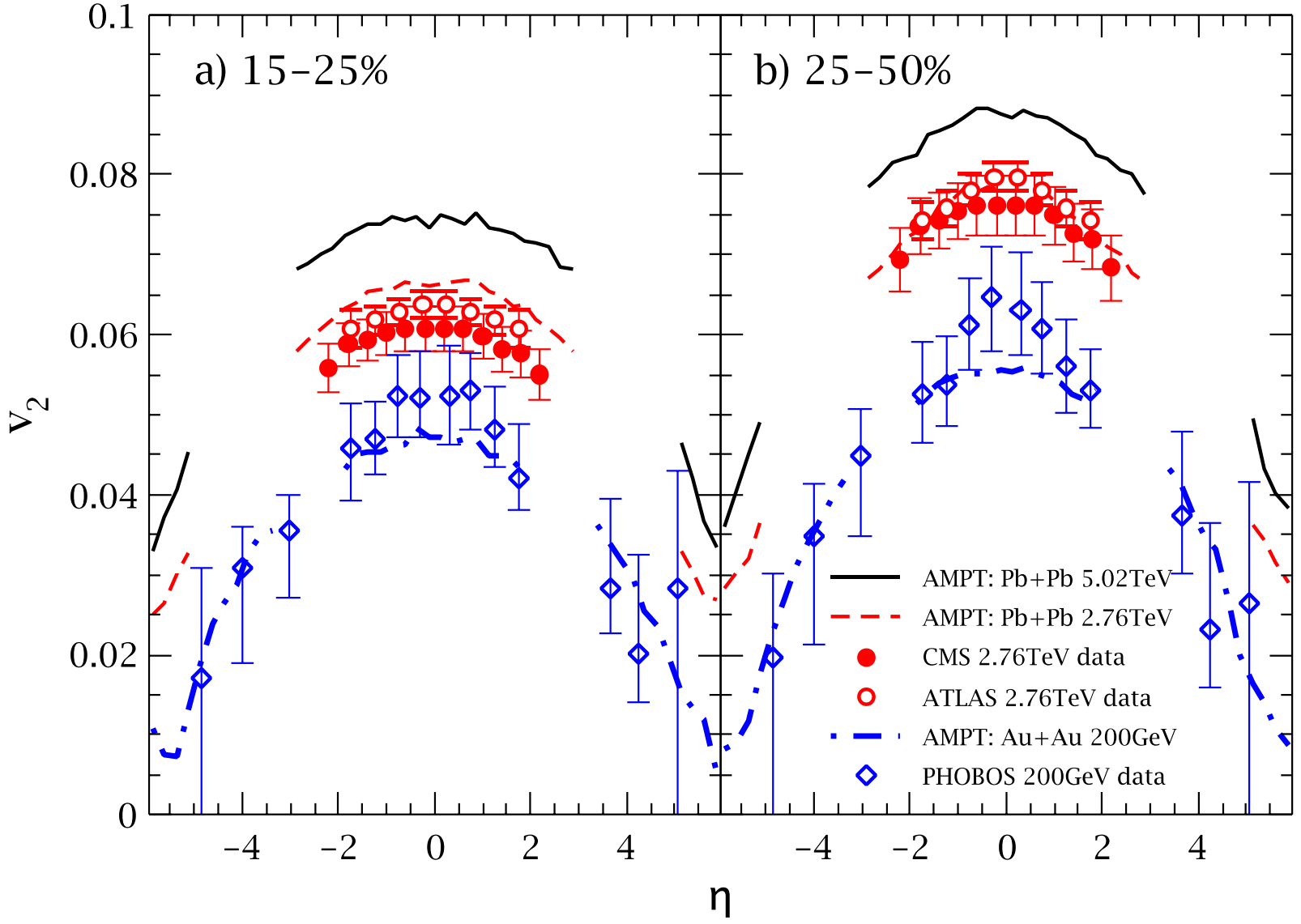

Selected results: predictions for 5ATeV Pb+Pb

Factorization ratio for v2 correlation:

$$r_n(\eta^a,\eta^b) \equiv \frac{V_{n\Delta}(-\eta^a,\eta^b)}{V_{n\Delta}(\eta^a,\eta^b)}$$

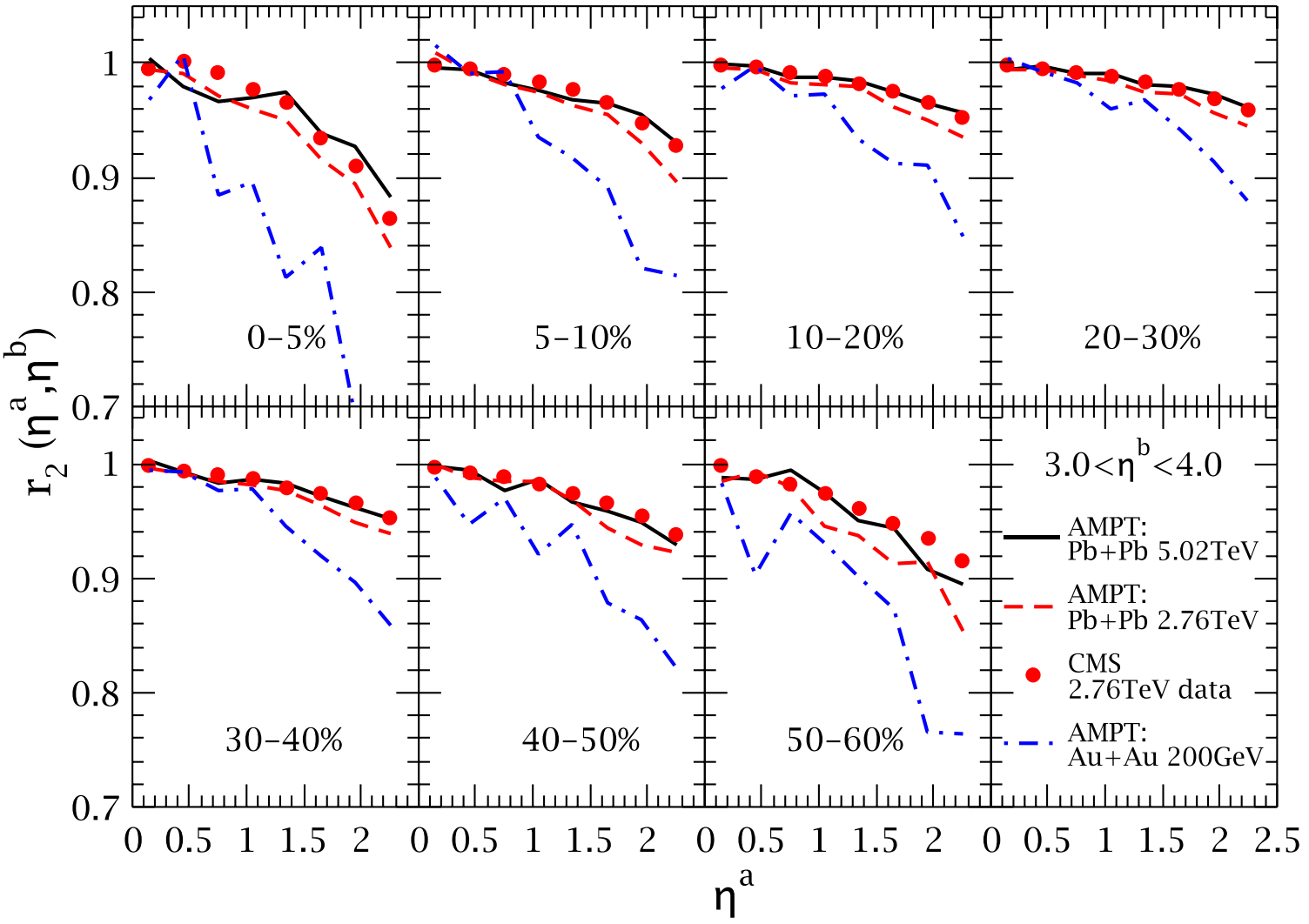

The initial spatial geometry including the event plane depends on η but also has longitudinal correlations. This comes naturally in the transport model: each wounded nucleon produces a tube of initial partons within a different (η_{min}, η_{max}) range at ~ the same transverse position.

Selected results: v_2 within jets

- By analyzing single jets that showers into many partons,

the CMS collaboration has observed a long range v_2^j for high-multiplicity jets in p+p collisions at 13 TeV;

this is not reproduced by PYTHIA or SHERPA model.

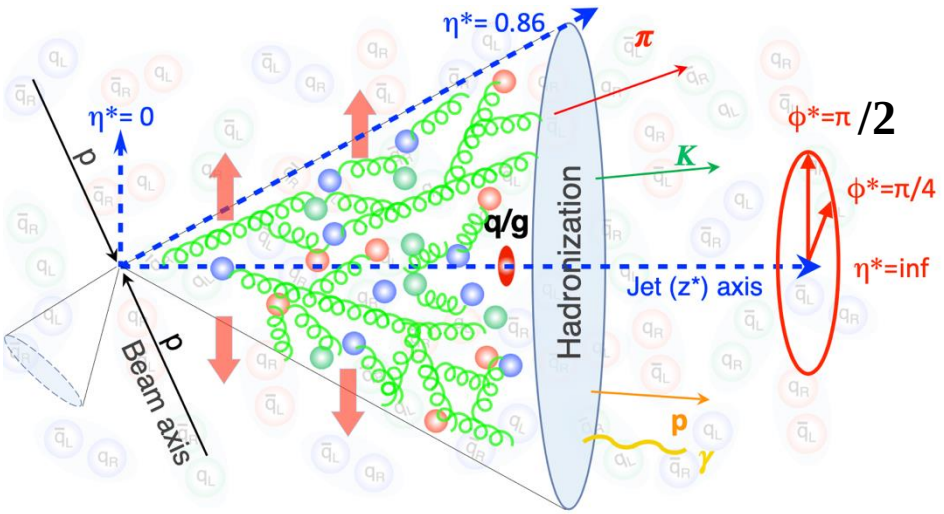

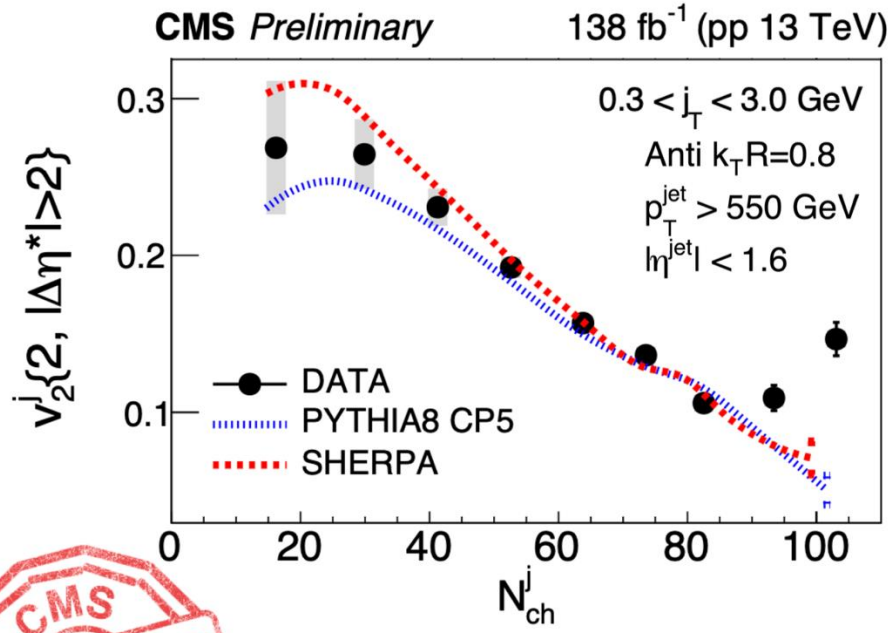

CMS Collaboration, 2312.17103

Selected results: v_2 within jets

We use the ZPC parton cascade to let shower partons scatter,
the hadronize with Lund string fragmentation, and enter UrQMD (hFSI).

Final state interactions enhance v_2^j at high N^j_{ch} (>70);

➡ parton interactions are necessary to reproduce the rising trend of v_2^j

W Zhao, ZWL & XN Wang, 2401.13137

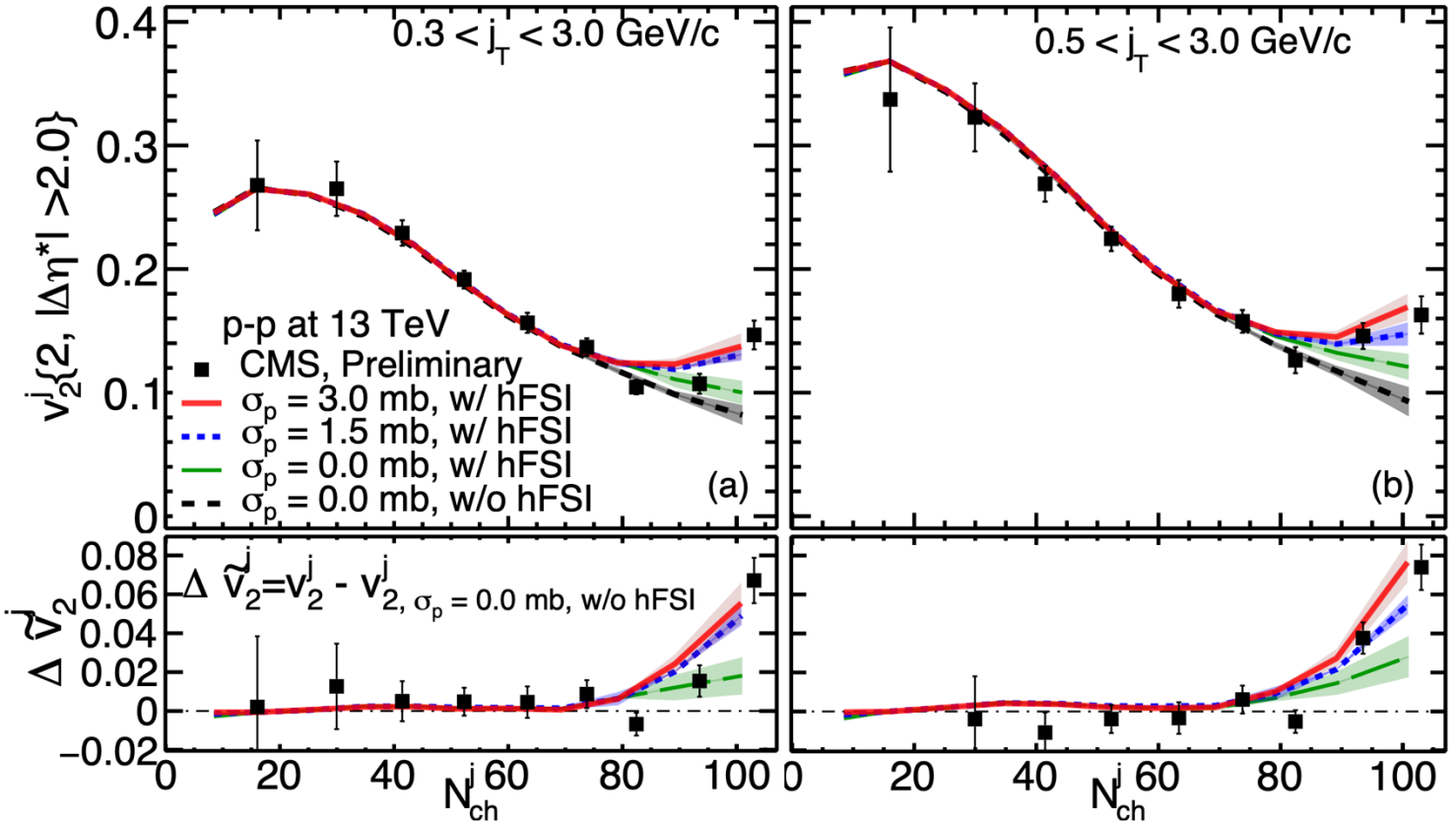

Selected results:

A detailed discussion on parton escape

- Flows can be dominated by non-equilibrium parton escape for finite systems/energies

L He et al. PLB 753 (2016);
ZWL at QM2015 & SQM2017;
HL Li et al. PRC 99 (2019)

Transport model for large systems

It has been commonly believed that:

- Transport models at large-enough cross section
  will approach hydrodynamics.

- Early hydro-type collective flow in sQGP
  converts initial spatial anisotropy into final momentum-space v_n

- For low-P_T particles in high-energy heavy ion collisions,
  since both hydrodynamics and transport models can describe v_n data,
  the mechanism of v_n development in transport models
  (via particle interactions)
  is in principle the same as in hydrodynamics *(via pressure gradients)*.

Transport model for small systems

Small systems: again, both hydrodynamics and transport can describe flow.

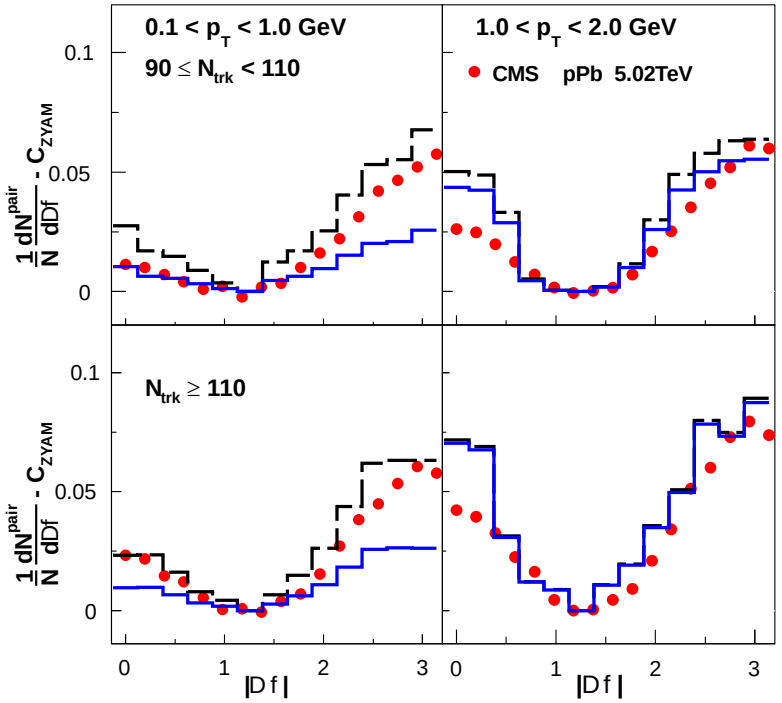

Bozek and Broniowski, PLB 718 (2013)
using e-by-e viscous hydrodynamics.

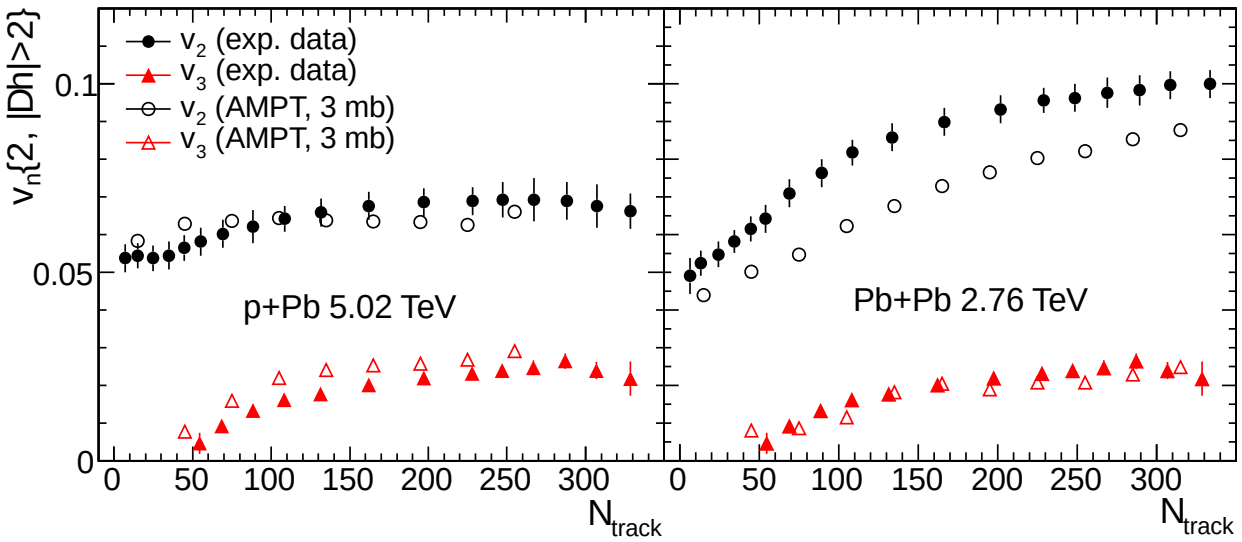

Bzdak and Ma, PRL 113 (2014)
using AMPT (String Melting version).

Questions for small systems such as p+Pb or d+Au or p+p:

- Mean free path may be comparable to the system size;
  is hydrodynamics still applicable to such small systems?
- Transport and hydrodynamics should be different for small systems,
  could they also be different for large systems?

The escape mechanism

We have followed the complete parton collision history and study the generation of parton v2 in AMPT. He et al. PLB 753 (2016)

Ncoll: *number of collisions suffered by a parton.*

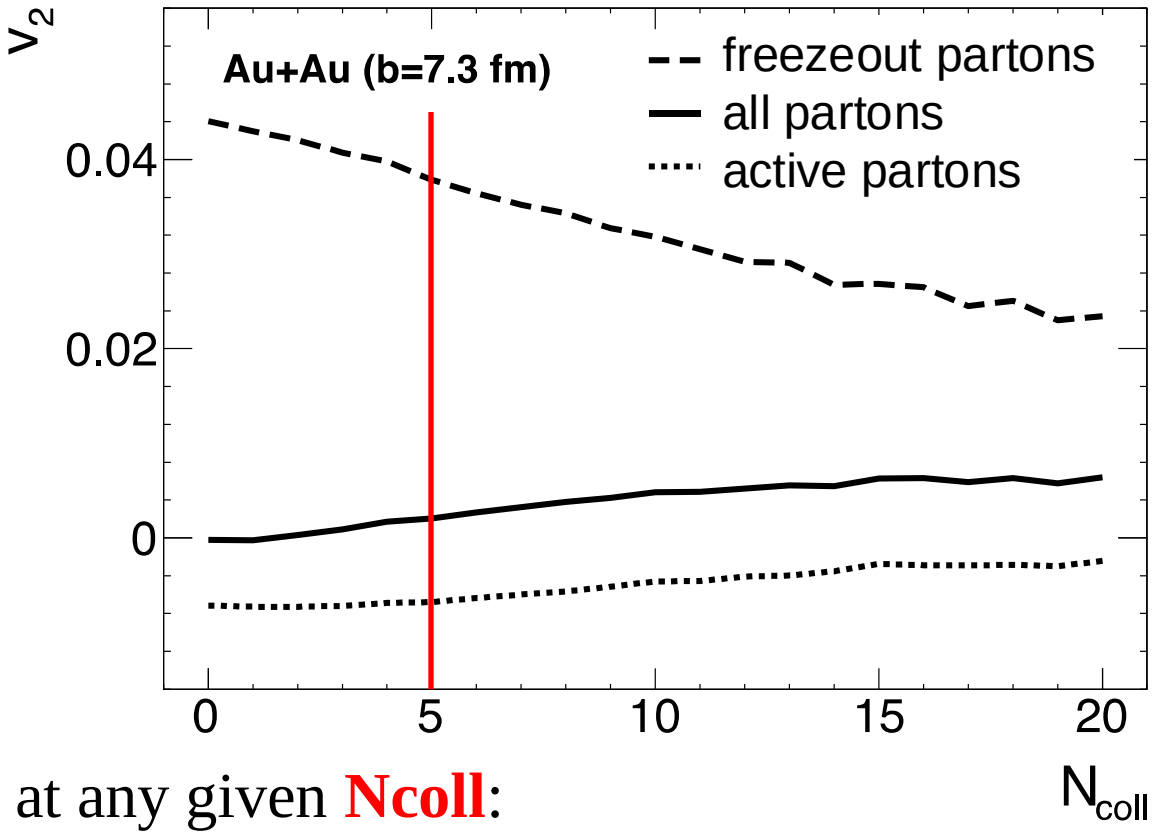

3 parton populations at any given **Ncoll**:

freezeout partons: *freeze out/hadronize after exactly **Ncoll** collisions;*

active partons: *will collide further, freeze out after >**Ncoll** collisions;*

all partons: *sum of the above two populations (i.e. all partons that have survived **Ncoll** collisions).*

At Ncoll=0:

all partons: $\mathbf{v_2=0}$ by symmetry (*since they include all initial partons*);

they contain 2 parts:

freezeout: $v_2 \approx 4.5\%$,

active: $v_2 < 0$.

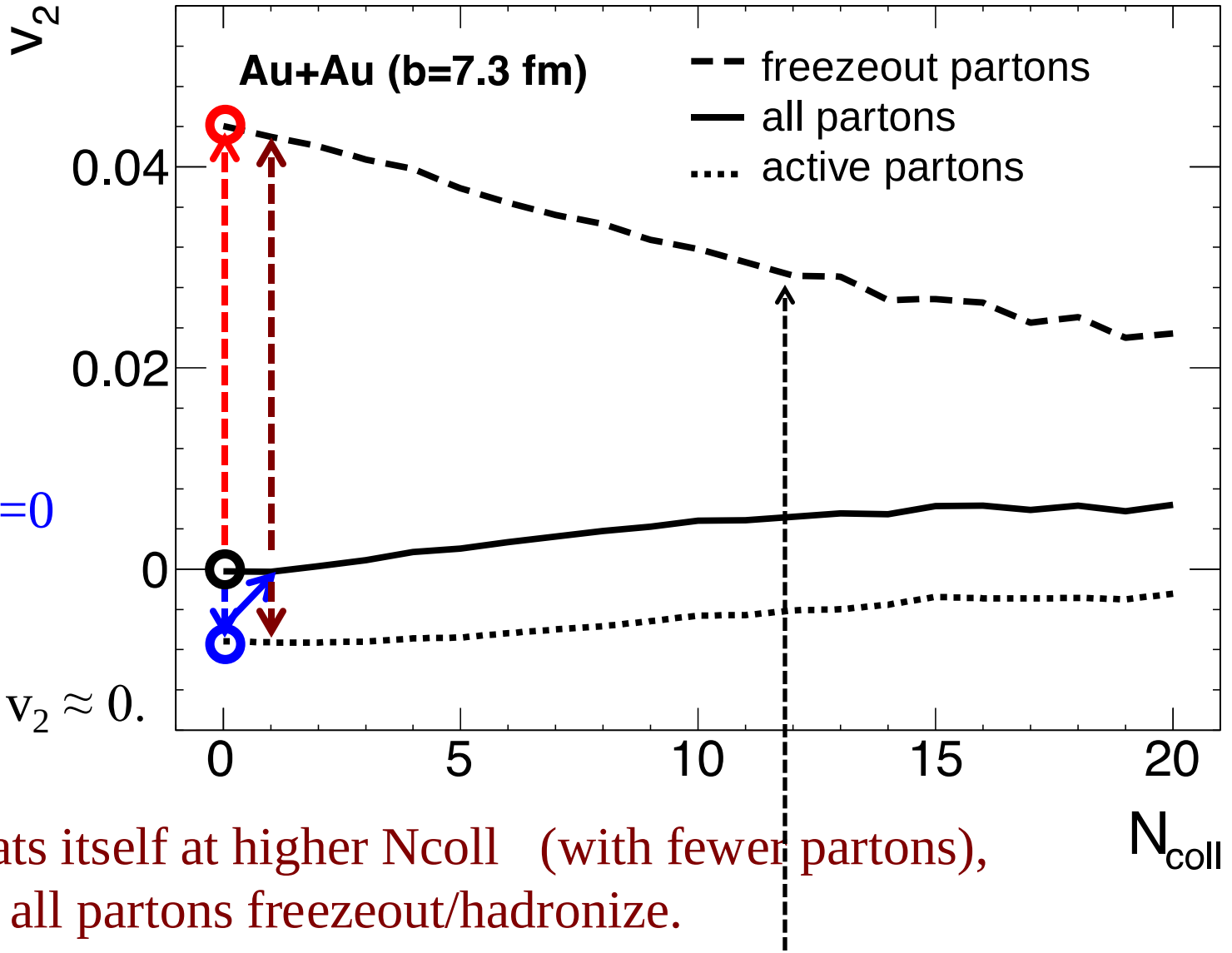

At Ncoll=1:

active partons at Ncoll=0 collide once each & become **all partons** at Ncoll=1: $v_2 \approx 0$.

This process repeats itself at higher Ncoll (with fewer partons), eventually all partons freezeout/hadronize.

<v2> = weighed average of the freezeout partons' v2 at different Ncoll.

At Ncoll=0:

escaped partons: $v_2 \approx 4.5\%$,

this is **purely** due to
anisotropic escape probability
(response to geometrical shape only,
no contribution from collective flow)

In simplified picture of elliptic flow:

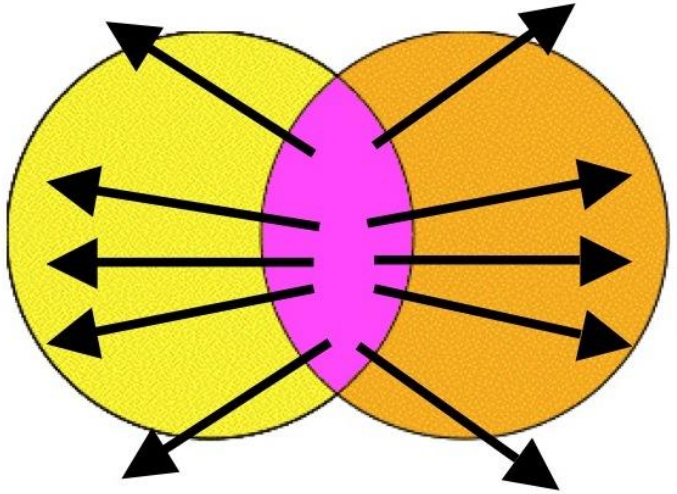

At Ncoll>=1:

escaped partons: $v_2 > 0$,

this is due to
anisotropic escape probability
& (anisotropic) **collective flow**.

How to separate the two contributions?

Final v_2 is generated by
interactions in presence of spatial anisotropy,
which also generate (anisotropic) collective flow.

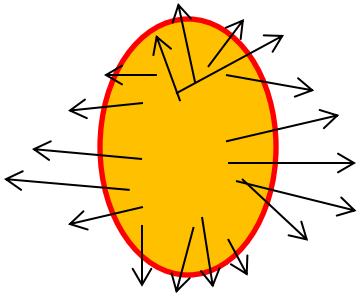

f(**x**,**p**,t)

Let's view v_2 as coming from 2 separate but complimentary sources:

1) Pure escape ("the escape mechanism"):

v_2 from spatial anisotropy only

if there were no collective flow,

this is due to anisotropic escape probability.

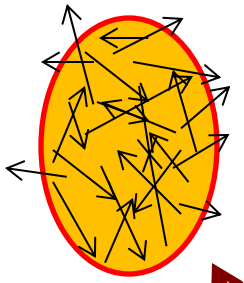

f(**x**,iso **p**,t)

2) Pure flow:

v_2 from anisotropic collective flow only

if there were no spatial anisotropy.

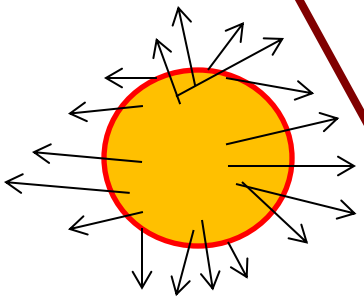

f(iso **x**,**p**,t)

The two are coupled in the actual evolution,
so we design a **random-ϕ test** to estimate contribution from **1):**

we randomize ϕ after each parton scattering to destroy collective flow.

$$\beta_\perp = \left\langle \frac{\vec{r}_\perp \cdot \vec{p}}{r_\perp \; p} \right\rangle$$

measures space-momentum correlation.

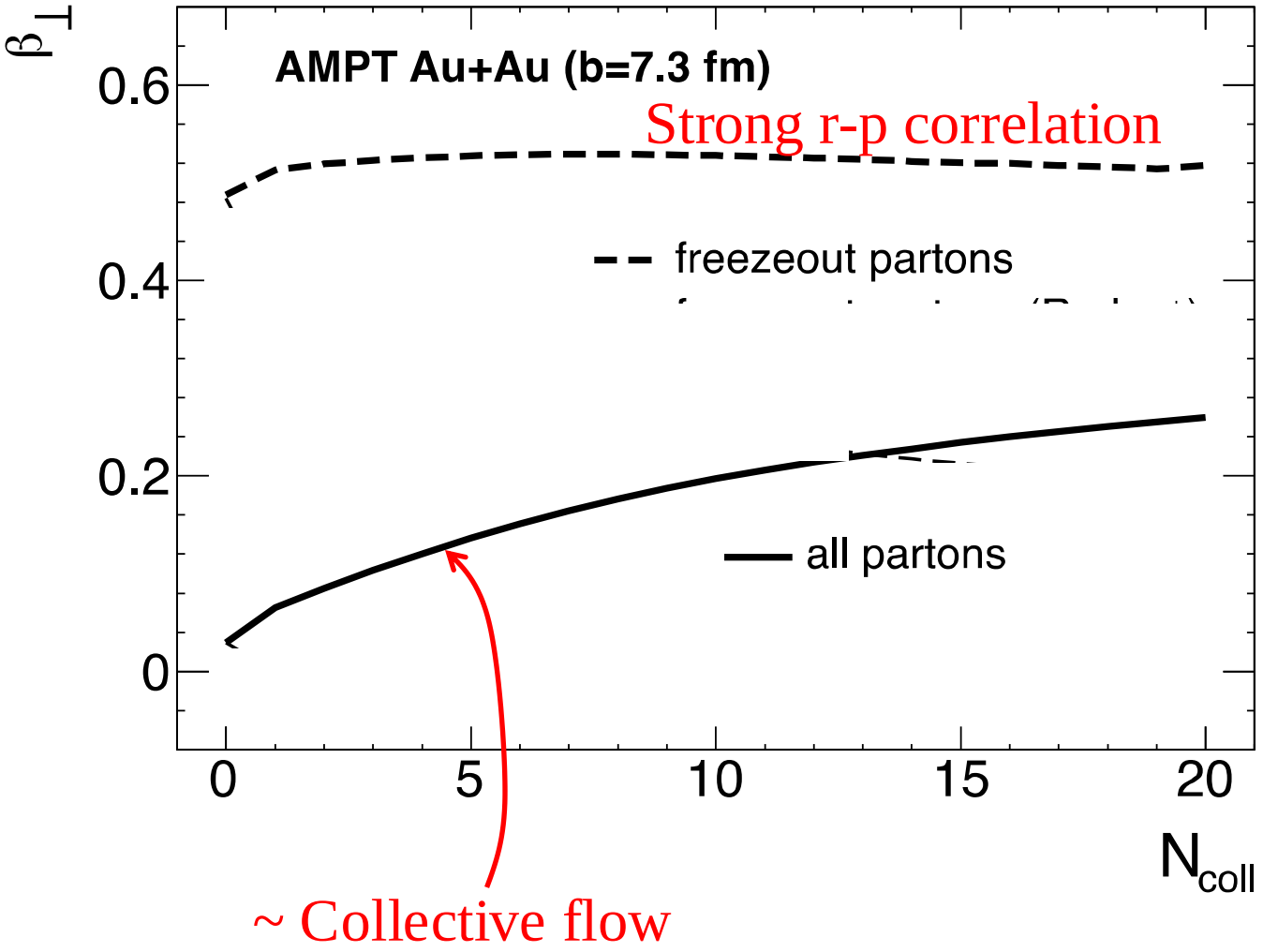

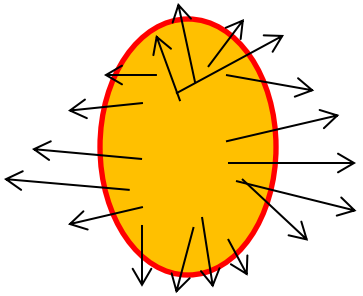

$$\beta_\perp = \left\langle \frac{\vec{r}_\perp \cdot \vec{p}}{r_\perp \; p} \right\rangle$$

measures space-momentum correlation.

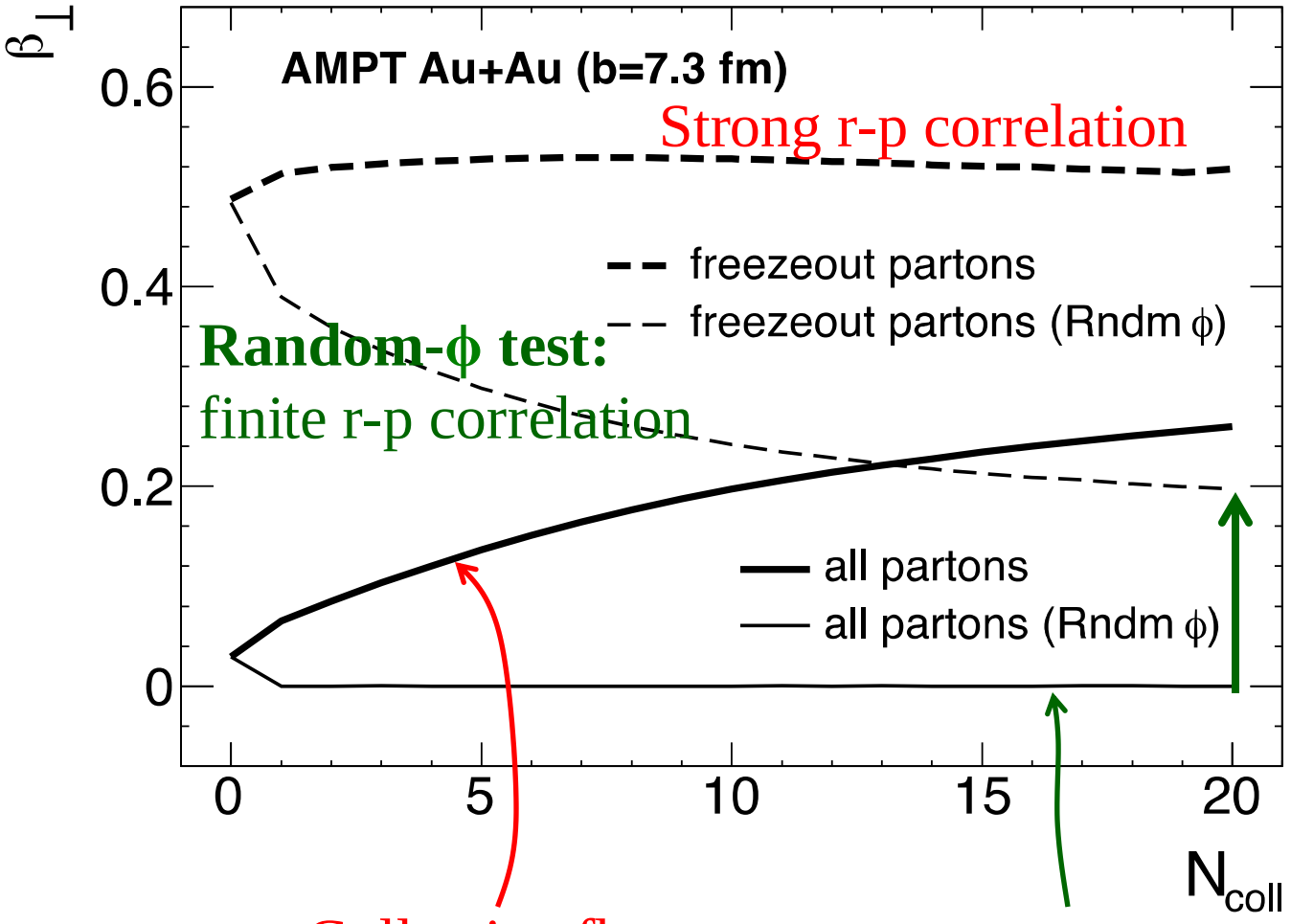

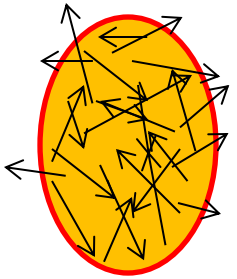

r-p correlation **purely from escape mechanism**, *not from collective flow*

v_2 from **Random Test:** purely from the escape mechanism

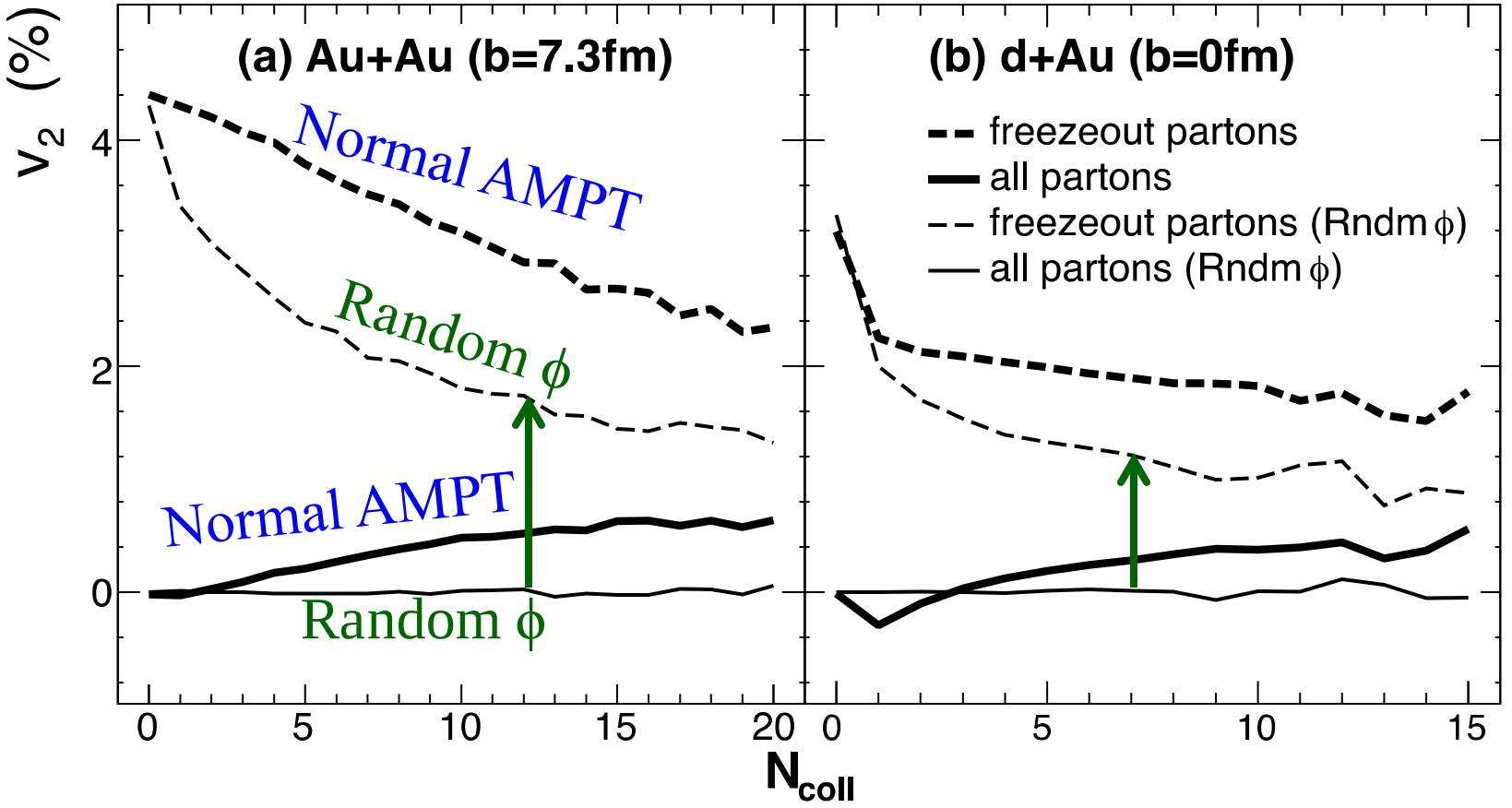

	Normal $\langle v_2 \rangle$	$\langle v_2 \rangle$ for random-ϕ	**Ratio** ~ % from pure escape	$\langle N_{coll} \rangle$
Au+Au	3.9%	2.7%	**69%**	4.6 (*modest*)
d+Au	2.7%	2.5%	**93%**	1.2 (*low*)

He et al. PLB753 (2016)

ZWL et al. NPA 956 (2016)

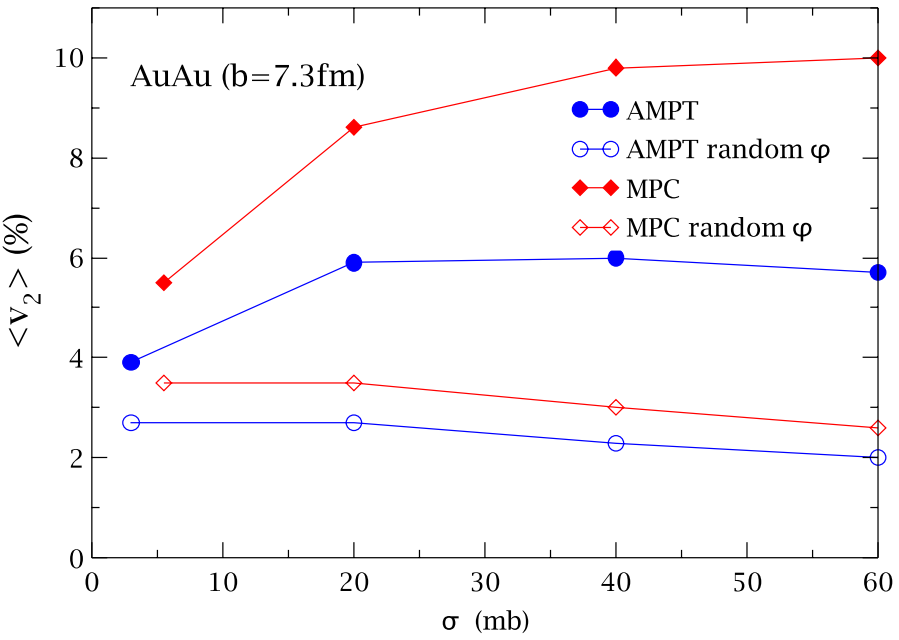

v_2 Ratio

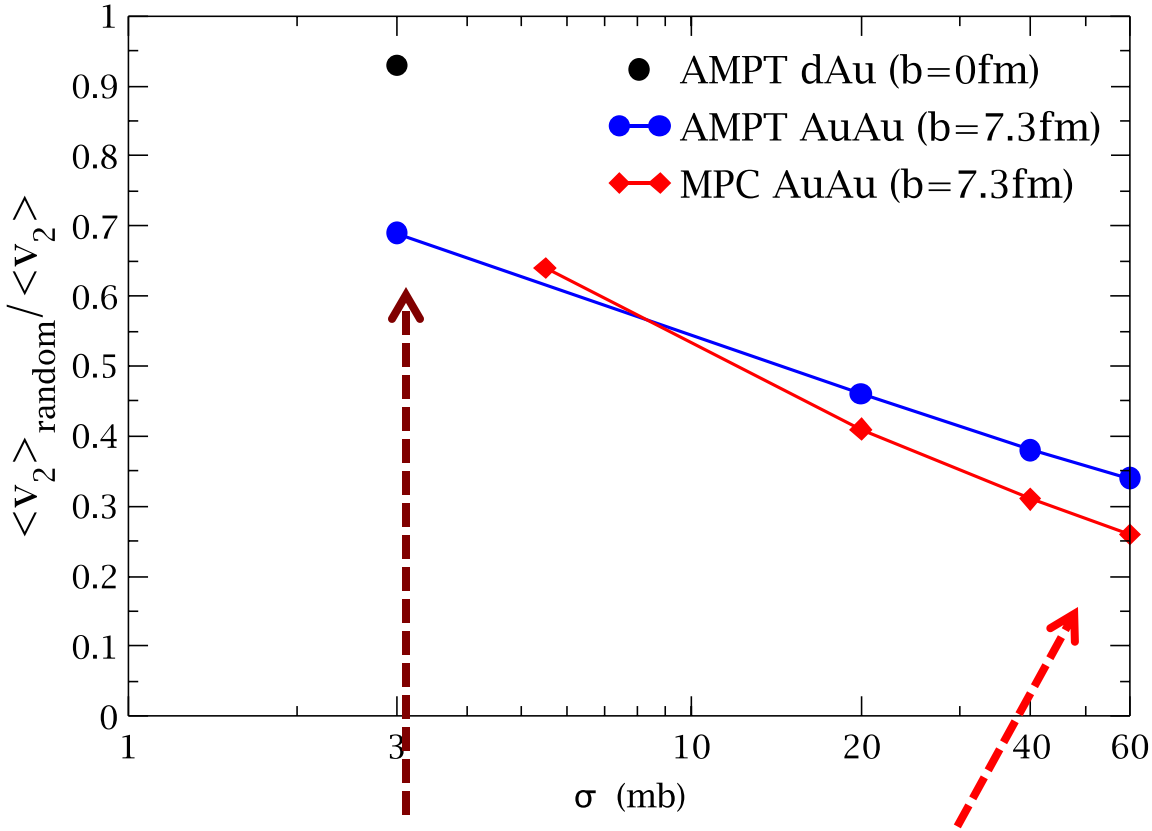

MPC: the same qualitative conclusion as AMPT

despite many differences (*parton initial condition, cross section & dσ/dt, formation time, parton-subdivision*)

Anisotropic particle escape is dominant contribution of v_2 for small systems & even for semi-central AuAu at RHIC

At very large σ or <Ncoll>, hydrodynamic collective flow will be the dominant contribution of v_2

- At low/modest opacity/<Ncoll>: transport and hydrodynamics are different.

The escape mechanism dominates v_n at low to modest opacity/<Ncoll>;
hydro-type collective flow dominates v_n at very high opacity/<Ncoll>:
which is the case for AA collisions?
which is case for pp or pA collisions?

- To better address questions about the collectivities in small systems:
  are they real signals from collectivity?
  are they from formation of a parton matter?
  is the small system far from or close to equilibrium?

transport models / kinetic theory are crucial as they address non-equilibrium dynamics.

Heiselberg & Levy, PRC (1999),
Borghini et al. EPJC (2018),
Kurkela et al. PLB (2018),
EPJC (2019), PRC (2019),
Kurkela, Törnkvist & Zapp, EPJC (2024), ...
KoMPoST, ALPACA

A tool for the heavy ion community

Triangular flow v3
was discovered with help of AMPT:
Alver & Roland, PRC 81 (2010)

What happens in an individual event:

A b=10fm Au+Au event at 200AGeV
from String Melting AMPT

Simplified picture of flow

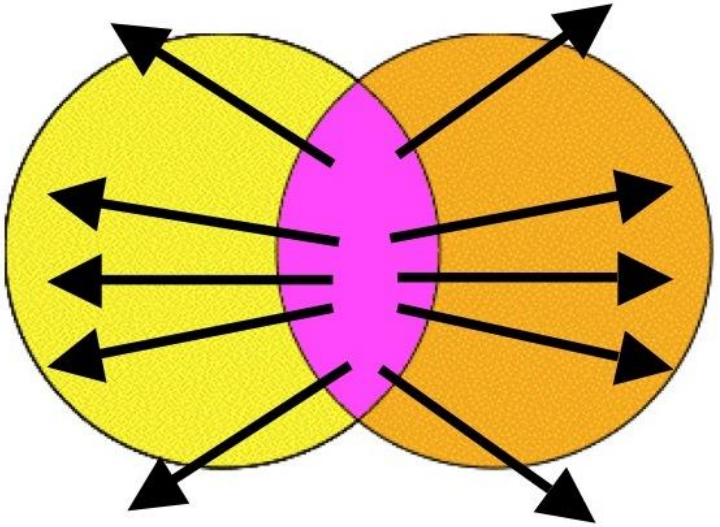

⊙
Beam axis

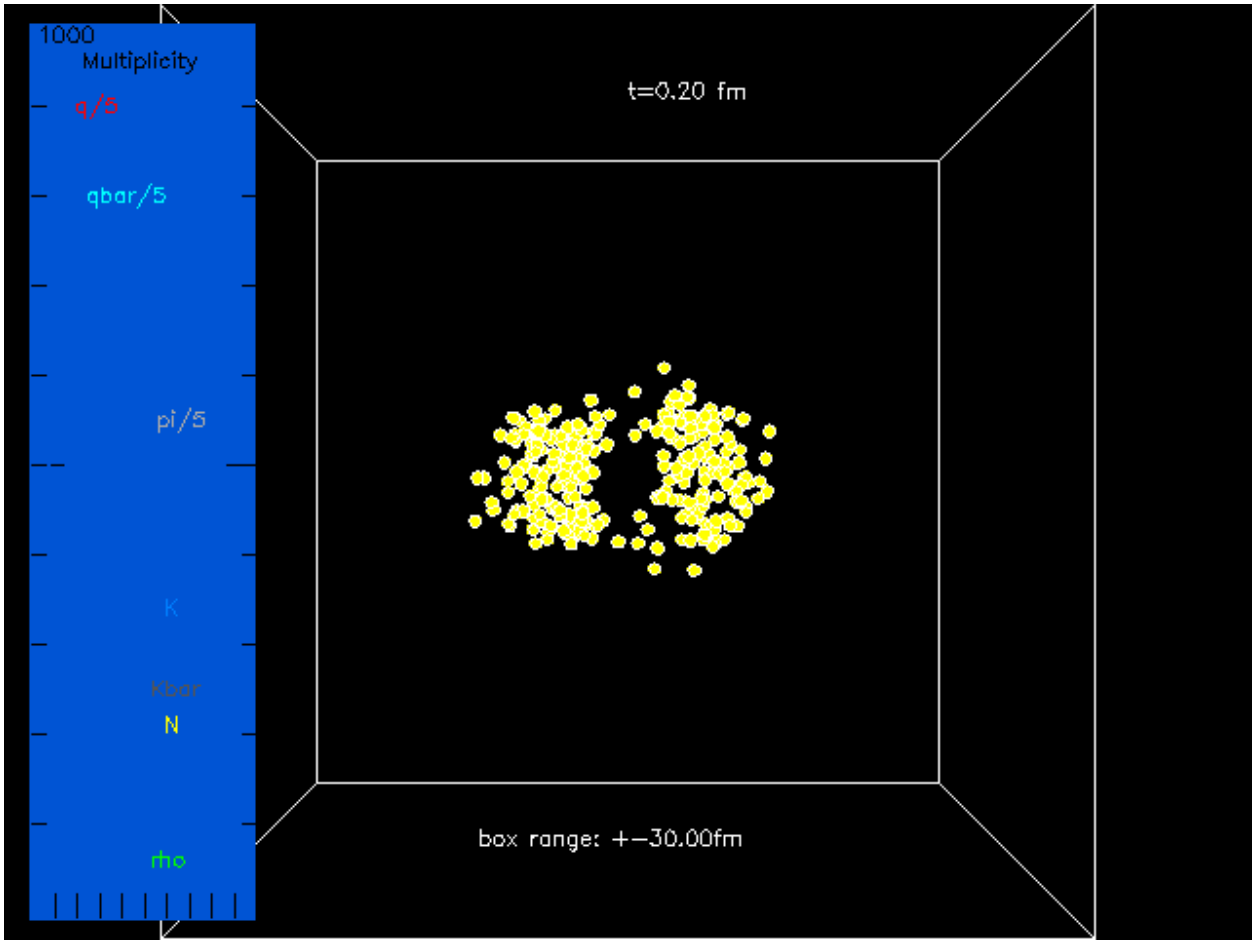

A tool for the heavy ion community

- Discovery of triangular flow v_3 — Alver & Roland, PRC 81 (2010)
- Longitudinal (de)correlations of flows — Pang et al. PRC 91 (2015) & EPJA52 (2016); ...
- Flows can be dominated by non-equilibrium parton escape for finite systems/energies — L He et al. PLB 753 (2016); ZWL at QM2015 & SQM2017; HL Li et al. PRC 99 (2019)
- CME signal & background — Shou, Ma & Ma, PRC 90 (2014); Huang, Ma & Ma, PRC 97 (2018); XL Zhao & Ma, PRC 106 (2022); Chen, Zhao & Ma, 2301.12076; ...
- Vorticity & polarization observables — Jiang et al. PRC 94 (2016); H Li et al. PRC 96 (2017); Lan et al. PLB 780 (2018); ...
- Incoming nuclei with nuclear structure — Haque, ZWL & Mohanty, PRC (2012); HJ Xu et al. PRL 121 (2018), CPC 42 (2018), HL Li et al. PRL 125 (2020); Jia, Giacalone & Zhang, PRL 131 (2023); ...

Challenges and opportunities

Some advantages of a Monte Carlo transport model

- Can address non-equilibrium dynamics:
  important for small collision systems
  & early time of large collision systems
  & heavy flavors in large collision systems

- Self-consistent chemical and kinetic freeze-out

- 3-dimensional production/distribution of energy/momentum and conserved charges (B, Q, S, C, ...)

- Contains explicit parton and hadron degrees of freedom

Challenges and opportunities

Some challenges for a Monte Carlo transport model

- Difficult to reproduce a given Equation of State
  with explicit parton and hadron degrees of freedom

- Difficult to reproduce a given shear viscosity at finite T
  with explicit parton interactions

- Many-body interactions may be necessary at very high densities,
  but difficult to implement

Challenges and opportunities

Transport model structure

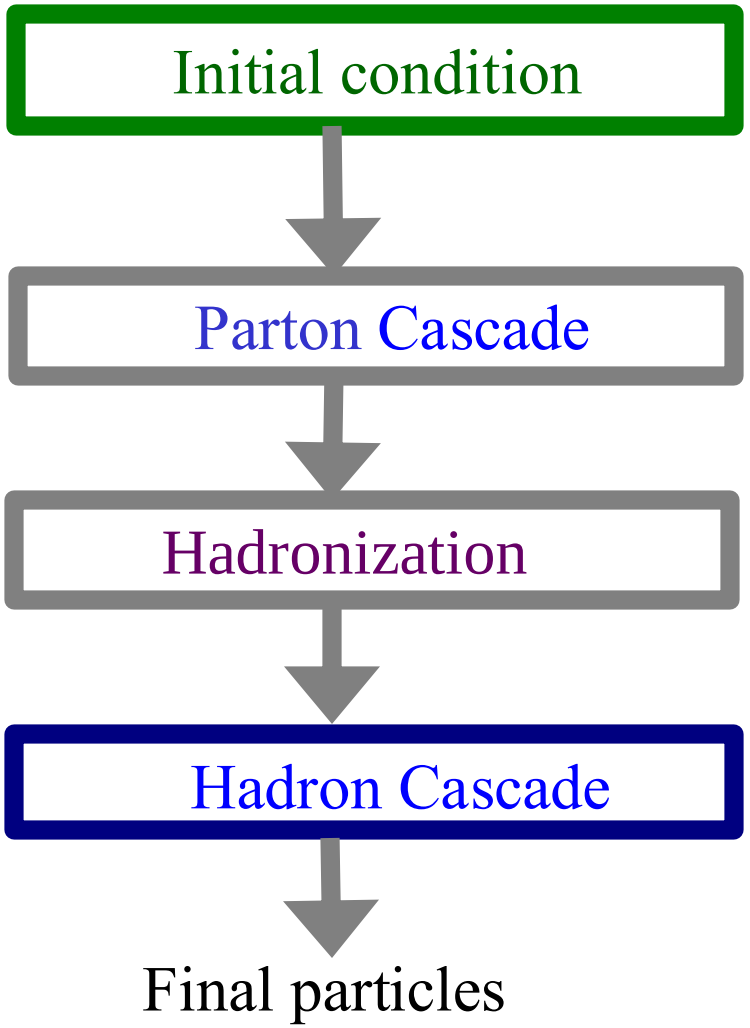

Opportunities for developments
(many not limited to transport models)

Nuclear structure/deformation/Nskin.
Finite nuclear crossing time/thickness.
Dynamical creation of parton matter.

Finite-temperature QCD/kinetic theory.
Transport under electromagnetic fields.

Spin transport.
Chiral phase transition.
Critical endpoint physics.
...